31. Ishiyama M, Miyazono Y, Sasamoto K, Ohkura Y and Ueno K: A highly water-soluble disulfonated tetrazolium salt as a chromogenic indicator for NADH as well as cell viability. Talanta 44: 1299-1305, 1997.
32. Steel GG and Peckham MJ: Exploitable mechanisms in combined radiotherapy-chemotherapy: the concept of additivity. Int J Radiat Oncol Biol Phys 5: 85-91, 1979.
33. Kondo M, Nagano H, Wada H, Damdinsuren B, Yamamoto H, Hiraoka N, Eguchi H, Miyamoto A, Yamamoto T, Ota H, Nakamura M, Marubashi S, Dono K, Umeshita K, Nakamori S, Sakon M and Monden M: Combination of IFN-alpha and 5-fluorouracil induces apoptosis through IFN-alpha/beta receptor in human hepatocellular carcinoma cells. Clin Cancer Res 11: 1277-1286, 2005.

CCR FOCUS

Molecular Mechanisms of Epidermal Growth Factor Receptor (EGFR) Activation and Response to Gefitinib and Other EGFR-Targeting Drugs

Mayumi Ono[1] and Michihiko Kuwano[2]

Abstract The epidermal growth factor receptor (EGFR) family of receptor tyrosine kinases, including EGFR, HER2/erbB2, and HER3/erbB3, is an attractive target for antitumor strategies. Aberrant EGFR signaling is correlated with progression of various malignancies, and somatic tyrosine kinase domain mutations in the *EGFR* gene have been discovered in patients with non–small cell lung cancer responding to EGFR-targeting small molecular agents, such as gefitinib and erlotinib. EGFR overexpression is thought to be the principal mechanism of activation in various malignant tumors. Moreover, an increased *EGFR* copy number is associated with improved survival in non–small cell lung cancer patients, suggesting that increased expression of mutant and/or wild-type EGFR molecules could be molecular determinants of responses to gefitinib. However, as *EGFR* mutations and/or gene gains are not observed in all patients who respond partially to treatment, alternative mechanisms might confer sensitivity to EGFR-targeting agents. Preclinical studies showed that sensitivity to EGFR tyrosine kinase inhibitors depends on how closely cell survival and growth signalings are coupled with EGFR, and also with HER2 and HER3, in each cancer. This review also describes a possible association between EGFR phosphorylation and drug sensitivity in cancer cells, as well as discussing the antiangiogenic effect of gefitinib in association with EGFR activation and phosphatidylinositol 3-kinase/Akt activation in vascular endothelial cells.

The epidermal growth factor receptor (EGFR) is a member of the erbB family of receptor tyrosine kinase proteins, which also includes HER2/*neu* (erbB2), HER3 (erbB3), and HER4 (erbB4). These receptors are composed of an extracellular ligand-binding domain, a transmembrane lipophilic domain, and an intracellular tyrosine kinase domain and, with the exception of HER2, all bind to receptor-specific ligands (Fig. 1A and B). Phosphorylation of the tyrosine kinase domain followed by homodimerization or heterodimerization between different receptors of the same family leads to protein activation (1). Receptor dimerization is promoted by ligand binding, high receptor density from overexpression, and mutations in the kinase domain. Protein activation on the cell surface of cancer cells is believed to promote signaling cascades, cell growth, differentiation, cell survival (apoptosis), drug and radiation sensitivity, cell cycle progression, and angiogenesis (Fig. 1A).

For cancer cells, various mechanisms of EGFR activation are now shown: overexpression of ligands and receptors, *EGFR* gene gain, and activating mutations. Under physiologic conditions, specific soluble ligands bind to the extracellular domains of EGFR, HER3, and HER4, but no ligand has been identified for HER2 (Fig. 1A). Of these ligands, EGF and transforming growth factor-α (TGF-α) selectively bind to EGFR, following dimerization as a homodimer or as a heterodimer with other members, and undergo autophosphorylation at specific tyrosine residues within the intracellular domain (Fig. 1B). This autophosphorylation activates downstream signaling pathways, including the Ras/Raf/mitogen-activated protein kinase pathway [extracellular signal-regulated kinase (ERK) 1/2], the phosphatidylinositol 3-kinase (PI3K)/Akt pathway, and the signal transduction and activator of transcription (STAT), and other pathways (Fig. 1A). ERK1 and ERK2 regulate cell growth and proliferation, whereas Akt as well as signal transduction and activator of transcription rather specifically regulate cell survival and apoptosis.

Recently, novel anticancer drugs targeting EGFR family members and other growth factor receptors have been developed. One of the EGFR tyrosine kinase inhibitors, gefitinib (Iressa), shows a highly specific affinity for EGFR and exerts its antitumor effects through inhibition of cell signaling(s) in cancer cells (2–4). EGFR and/or HER2 are highly expressed in many tumor types of epithelial origin, including breast, head and neck, bladder cancers, and non–small cell lung cancer (NSCLC; ref. 3). Expression of high levels of EGFR and/or HER2 has been associated with a poor prognosis, especially in NSCLC patients (5).

The discovery of *EGFR* mutations with or without gene gain has enabled an understanding of how to treat certain NSCLC

Authors' Affiliations: [1]Department of Medical Biochemistry, Graduate School of Medical Sciences, Kyushu University, Fukuoka, Japan and [2]Research Center for Innovative CancerTherapy, Kurume University, Kurume, Japan
Received 3/16/06; revised 8/29/06; accepted 9/25/06.
Requests for reprints: Mayumi Ono, Department of Medical Biochemistry, Graduate School of Medical Sciences, Kyushu University, 3-1-1 Maidashi, Higashi-ku, Fukuoka, 812-8582, Japan. Phone: 81-92-642-6098; Fax: 81-92-642-6203; E-mail: mayumi@biochem1.med.kyushu-u.ac.jp.

doi:10.1158/1078-0432.CCR-06-0646

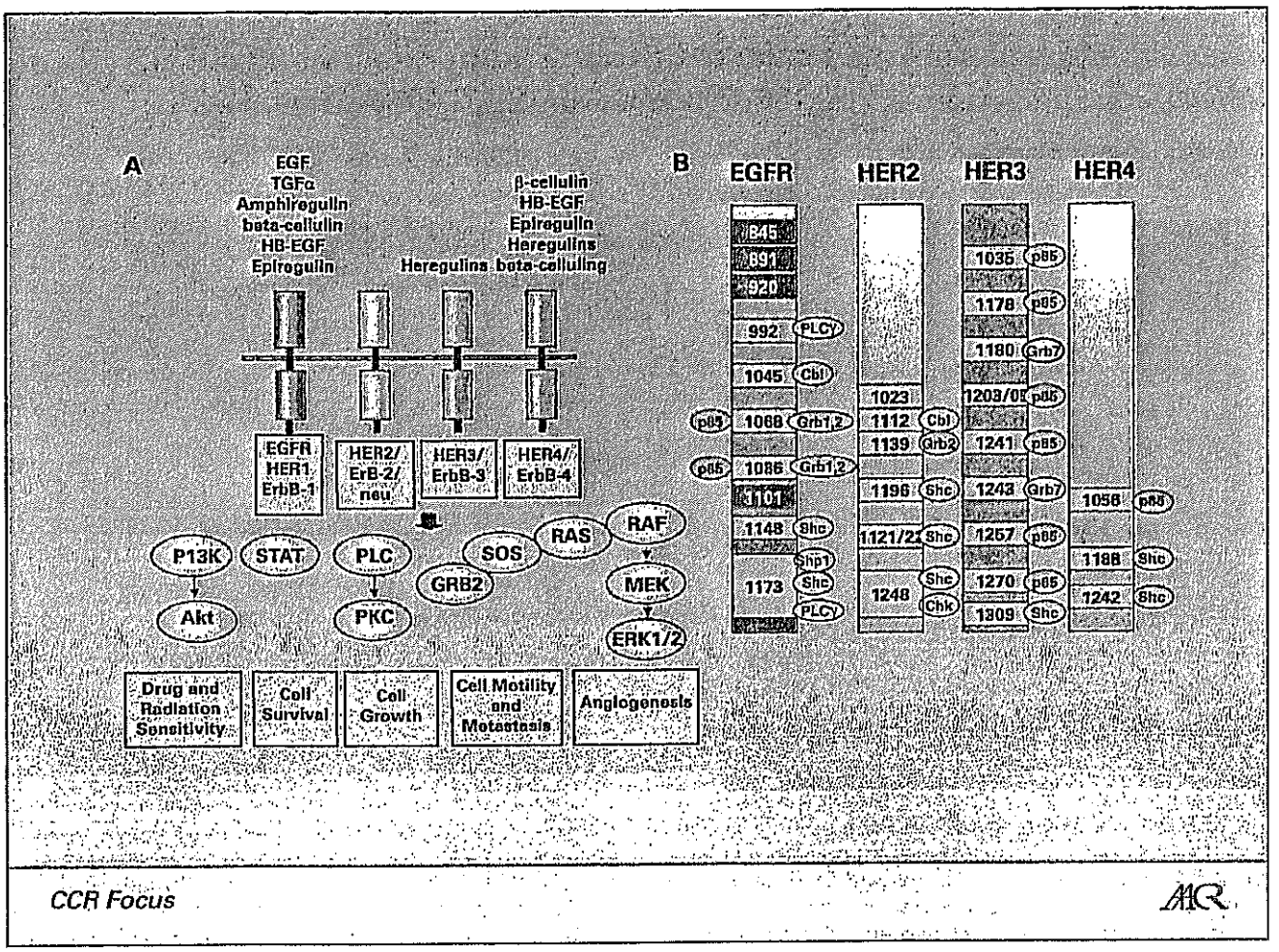

Fig. 1. *A*, the EGFR family and its downstream signaling molecules as targets for cancer therapy. EGFR family proteins and their ligands. *B*, EGFR family proteins, their specific phosphorylation sites, and binding sites of signaling molecules to the tyrosine kinase domains. Binding sites for PI3K (p85α) are found in EGFR, HER3, and HER4 but not in HER2.

patients with EGFR-targeting drugs from the standpoint of evidence-based therapeutic strategies. NSCLC patients responding to gefitinib or another EGFR-targeting drug, erlotinib, often carry various somatic mutations in the *EGFR* gene (4). Most of the identified mutations are located within exons 18 to 21, as activating EGFR mutations. A point mutation in exon 21 (L858R) and a deletion mutation in exon 19 (del E746-T751) offer a predictive marker for improved therapeutics with gefitinib or erlotinib. Moreover, the extent of *EGFR* gene gain also plays a critical role in the therapeutic efficacy of such drugs (6). However, it is also known that not all patients with *EGFR* mutations or gene gains are susceptible to EGFR-targeting drugs (6–10). Successful therapy by such EGFR-targeting drugs could be expected for patients whose *EGFR* family members are amplified, mutated, or overexpressed in cancer cells (11). In this article, we will discuss how the EGFR family of proteins could be specifically associated with drug sensitivity or the therapeutic efficacy of EGFR-targeting drugs.

Activation of EGFR Downstream Signaling Molecules, *K-ras* Mutation, and EGFR Gene Gain

EGFR mutation or *EGFR* gene gain is associated with a more favorable outcome following treatment with EGFR-targeting drugs, such as gefitinib or erlotinib (6, 12). In preclinical studies, we discovered that drug sensitivity to gefitinib is closely correlated with EGFR-dependent ERK1/2 and Akt activation (13). PC9, which harbors a deletion (del 746-750) in exon 19 of *EGFR*, was shown to be the most sensitive of nine lung cancer cell lines to growth inhibition by gefitinib and showed the closest coupling of growth arrest and Akt/ERK1/2 activation inhibition (Fig. 2A and C). Consistent with this finding, Paez et al. (8) reported that the lung cancer cell line H3255 harboring the L858R mutation in *EGFR* exon 21 was also highly sensitive to gefitinib (Fig. 2B and C) and also that both Akt and ERK1/2 pathways in H3255 were highly susceptible to the inhibitory effect of gefitinib. Increasing drug sensitivity to gefitinib of cancer cells harboring

mutant EGFRs thus depends on how closely EGFR-driven signaling pathways (ERK1/2, Akt, and signal transduction and activator of transcription) are coupled with cell survival (apoptosis) and cell growth.

To understand in more detail which EGFR-driven signaling is specifically responsible for gefitinib-induced cytotoxicity and therapeutic efficacy, Sordella et al. (14) generated isogenic cell lines that expressed either wild-type (WT) EGFR or mutant EGFRs (L858R and del 746-750). Mutant EGFR selectively activated Akt and STAT 5 signaling, but not ERK1/2, to promote cell survival in lung cancer cells. Immunohistochemical analysis on advanced NSCLC showed

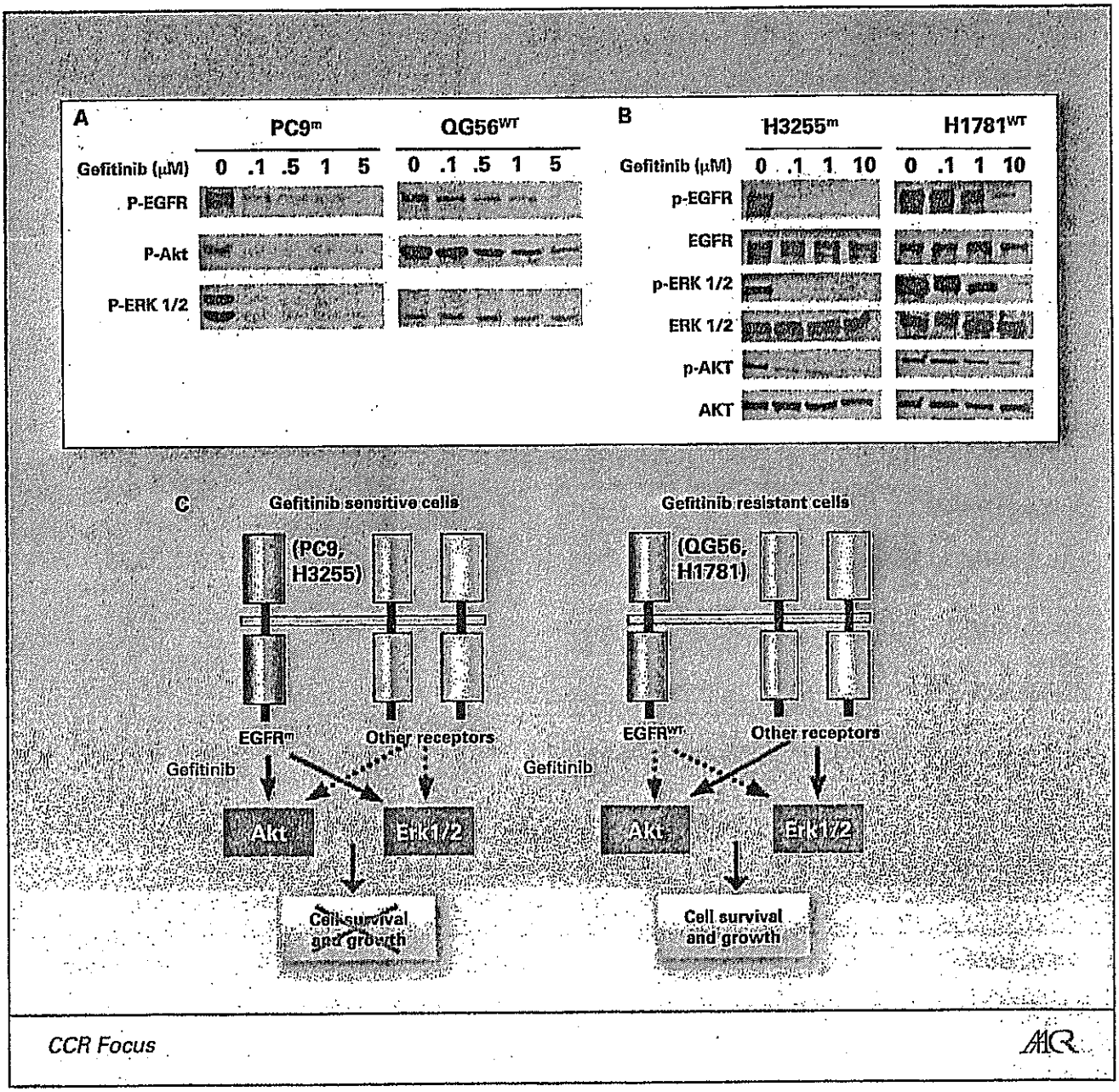

Fig. 2. *A* and *B*, comparison of the inhibitory effects of gefitinib on activation of EGFR, Akt, and ERK1/2 between gefitinib-sensitive NSCLC lines (PC9 and H3255) and gefitinib-resistant NSCLC lines (QG56 and H1781): $PC9^{m}$ and $H3255^{m}$ harbor *EGFR* mutations del E746-A750 and L858R, respectively, whereas $QG56^{WT}$ and $H1781^{WT}$ carry WT EGFR. *C*, a model showing how gefitinib sensitivity is controlled. In gefitinib-sensitive cell lines (PC9 and H3255), only EGFR-driven signaling dominates following Akt and ERK1/2 activation for survival and growth. In gefitinib-resistant lines (QG56 and H1781), EGFR is not a survival factor and other receptors or signals could dominate. $EGFR^{WT}$, WT EGFR; $EGFR^{m}$, activated mutant EGFR. Figure 2B is modified and adapted with permission from Science (8).

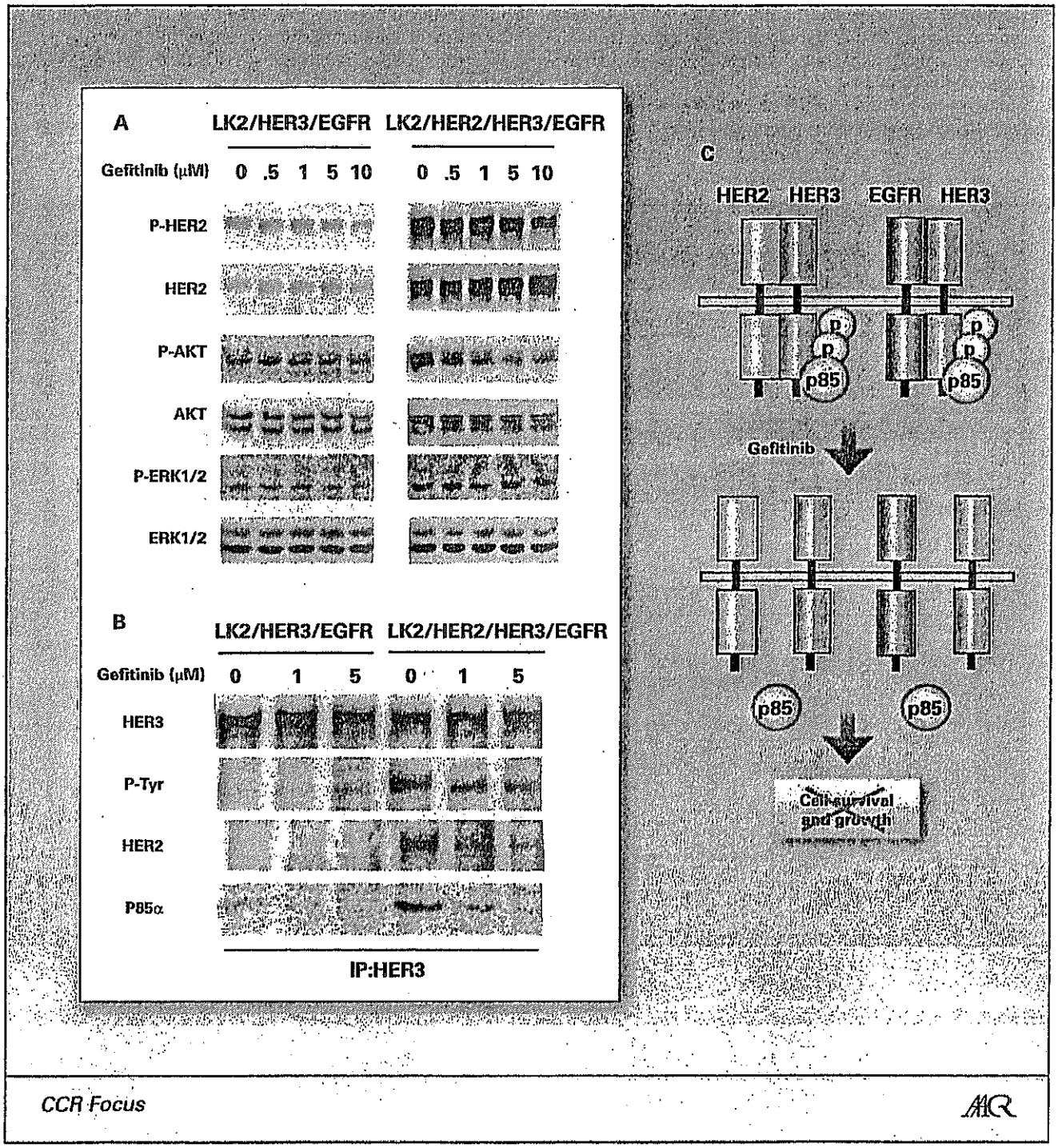

Fig. 3. Formation of the HER2/HER3 or the EGFR/HER3 heterodimer enhances both PI3K/Akt activation and cellular sensitivity to EGFR-targeting drugs, including gefitinib. *A*, EGFR-targeting drugs preferentially inhibit Akt phosphorylation in a dose-dependent manner in LK2/HER2/HER3/EGFR cells but not in LK2/HER3/EGFR cells. *B*, gefitinib inhibits the formation of HER2/HER3 heterodimers, the association of HER3 with p85α, and the concomitant inhibition of HER3 tyrosine phosphorylation in LK2/HER2/HER3/EGFR cells. *C*, hypothetical model showing how overexpression of EGFR family proteins confers cellular sensitivity to EGFR-targeting drugs. In addition to experimental data of (*A*) and (*B*; ref. 30), coexpression of HER3 with HER2 and/or EGFR was shown to confer gefitinib sensitivity to cancer cells (13, 26, 34). HER3 also mediated PI3K/Akt activity through heterodimer formation with EGFR (WT and mutant type) in gefitinib-sensitive cancer cells but not in gefitinib-resistant cells (34). In this model, heterodimer formation of HER2/HER3 or EGFR/HER3 activates PI3K/Akt pathway that plays a pivotal role in drug sensitivity to EGFR-targeting drugs.

that patients with phosphorylated AKT–positive tumors have a better response rate, disease control rate, and time to progression than patients with phosphorylated AKT–negative tumors when treated with gefitinib (15). The Akt signaling pathway activated by EGFR harboring activating mutations or gene gain is rather more specifically involved in enhanced drug sensitivity and therapeutic efficacy than the ERK1/2 pathway, suggesting phosphorylated AKT as one of the molecular determinants of response to EGFR-targeting drugs. However, further study is required to determine how phosphorylated AKT expression can be applied to determination of the clinical therapeutic efficacy of gefitinib (16). Furthermore, recent studies showed that NSCLC patients with a EGFR mutation of del 746-750 had a longer median survival than patients with the L858R point mutation when treated with gefitinib or erlotinib (17, 18), suggesting some differences in activating EGFR signaling by each EGFR mutation.

K-ras is a downstream mediator of EGFR-induced cell signaling, and *ras* mutations confer constitutive activation of the signaling pathways without EGFR activation. Growing evidence indicates that *K-ras* mutations are important in the development of lung carcinomas (19). Pao et al. (20) examined 60 lung adenocarcinoma patients and showed that *K-ras* mutations are associated with a lack of sensitivity to gefitinib or erlotinib. *K-ras* mutations seem to be resistant to EGFR-targeting agents and are reported to be mutually exclusive to *EGFR* or *HER2* gene mutations (21).

Increased *EGFR* gene gain is closely associated not only with gefitinib sensitivity but also with improved survival following gefitinib treatment in patients with advanced bronchoalveolar carcinoma (6, 22). *EGFR* gene gain is often observed in lung

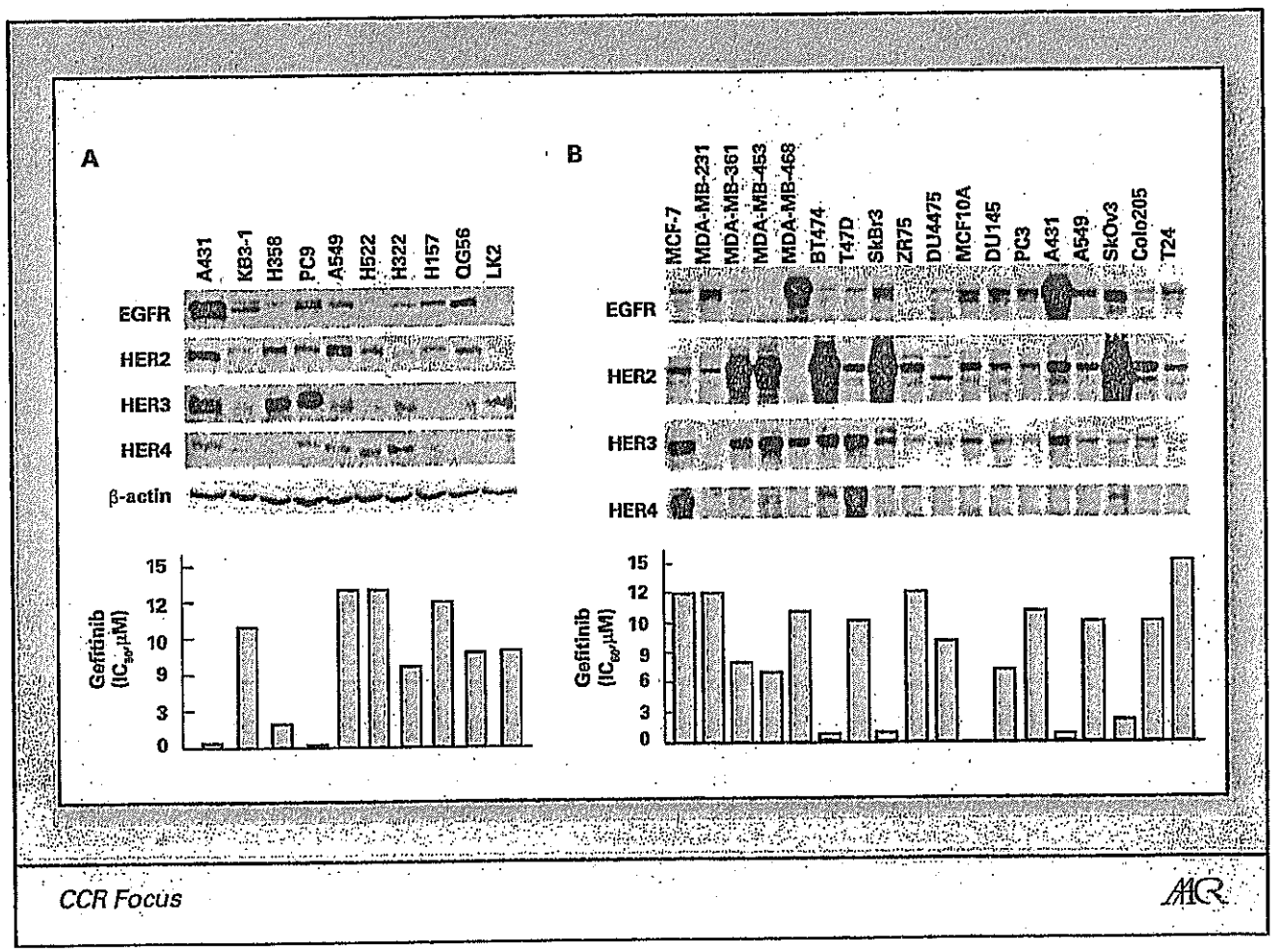

Fig. 4. Correlation of the expression of four EGFR family members with drug sensitivity to gefitinib in human cancer cell lines. Western blot analysis was done using 50 μg total cellular protein, and growth inhibition assays were done using various concentrations of gefitinib in culture. Average IC_{50} values (μm) are presented from duplicate experiments. *A*, human cancer cell lines contain various lung cancer lines and two epidermoid carcinoma cell lines (A431 and KB3-1). Modified with permission (13). *B*, human cancer cell lines contain mainly breast cancer lines and other cell lines derived from various tumor types. Modified with permission (25).

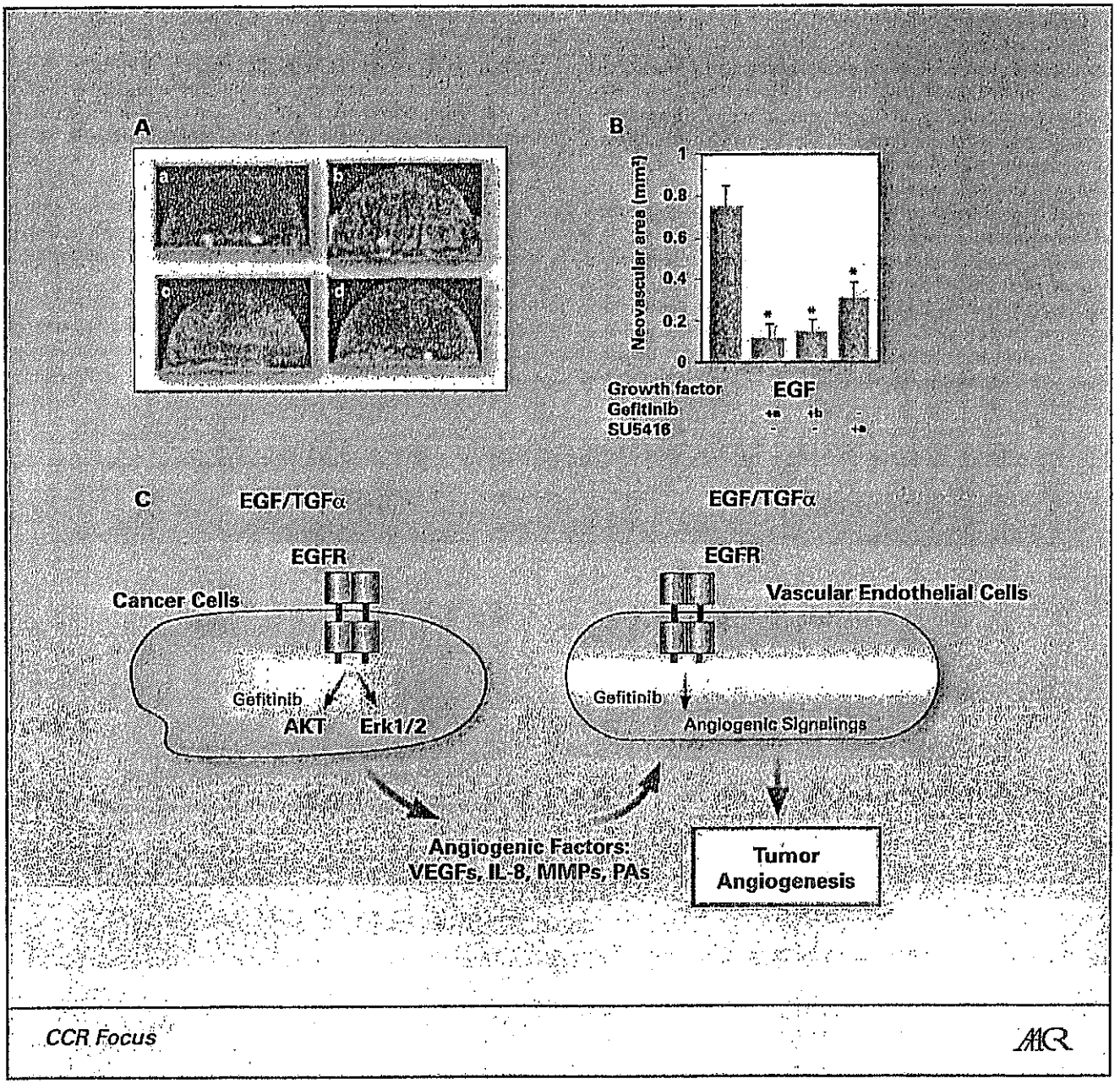

Fig. 5. Inhibition of angiogenesis is also responsible for the antitumor effect of gefitinib. *A*, angiogenesis induced by EGF in mouse corneas is inhibited by gefitinib and partially by SU5416. a, hydron alone, control; b, EGF (200 ng); c, EGF with gefitinib (50 mg/kg/d, i.p.); d, EGF with SU5416 (25 mg/kg/d, i.p.). *B*, quantification of corneal neovascularization in mice after treatment with gefitinib or SU5416. a, drug administered i.p.; b, drug administered in pellet. *, $P < 0.05$, significant difference from value for EGF alone. *C*, a model of EGF/TGF-α–induced angiogenesis and gefitinib inhibition of the tumor angiogenesis process. Cancer cells often produce TGF-α, which induces the production of potent angiogenic factors, VEGFs, interleukin-8 (*IL-8*), matrix metalloproteinases (*MMP*), plasminogen activators (*PA*), platelet-derived growth factors (*PDGF*), and other factors. EGF/TGF-α also directly activates EGFR in endothelial cells both in normal vessels and in tumor neovasculatures, which induce angiogenesis. Inhibition sites of gefitinib are indicated, suggesting that dual pathways are affected by gefitinib.

cancers, and increased copy number is more frequently seen in patients harboring *EGFR* mutations than those with the WT gene. Although the response rate to gefitinib for patients harboring mutations was 82%, it should be noted that amplified WT EGFR was also associated with responses in some 11% of patients (23). Patients with an amplified mutant allele are thus expected to receive more benefit from gefitinib than those with an amplified WT allele (10, 23).

HER2 and Other EGFR Family Proteins

HER2 as well as EGFR is highly expressed in several solid tumors. For example, overexpression of the HER2 protein was reported in 20% to 30% of breast cancers, and EGFR is also overexpressed in ~40%. *HER2* gene gain has been reported to be an independent predictive marker for overall survival and disease-free survival in node-positive patients (24). One representative molecular targeting drug is the human monoclonal antibody against HER2, trastuzumab (Herceptin), which improves the outcome of HER2-positive breast cancer. HER2 overexpression in various cancer cell lines or tumor xenografts also increases cytotoxicity and/or the antitumor effects of gefitinib (25, 26). In NSCLC patients, Cappuzzo et al. (27) reported that an increased *HER2* gene gain is associated with gefitinib sensitivity in EGFR-positive patients. Those patients whose tumors had high *HER2* copy number and *EGFR* mutation had the best objective response (53.8%) and disease control rate (76.9%), suggesting that HER2 fluorescence *in situ* hybridization analysis is a valuable method for selecting patients for tyrosine kinase inhibitor therapy. On the other hand, activating *HER2* mutations, including an exon 20 point mutation (G776L), have been reported in lung adenocarcinomas (28). A NSCLC patient harboring mutations in both HER2 (G776L) and EGFR (A859T) experienced a response after treatment with trastuzumab, despite disease progression after prior tyrosine kinase inhibitor therapy (29). Both *HER2* gene gain and mutation thus might be critical for cancer cell survival in NSCLC.

Although HER3 is unique among the EGFR family because it lacks tyrosine kinase activity, its six tyrosine phosphorylation sites effectively couple the protein to the PI3K/Akt pathway by providing excellent binding sites for PI3K (Fig. 1). In a preclinical study, we established HER2-overexpressing cell lines that express HER3 and very low levels of EGFR (LK2/HER2/HER3/EGFR), and these HER2 transfectants showed increased sensitivity to growth inhibition by gefitinib. Gefitinib preferentially inhibited phosphorylated AKT in LK2/HER2/HER3/EGFR cells, whereas phosphorylated ERK1/2 was not inhibited in either LK2/HER3/EGFR or LK2/HER2/HER3/EGFR cells. This is suggestive of selective inhibition of Akt activation by gefitinib (Fig. 3A; ref. 30). HER3 efficiently recruits the regulatory subunit of PI3K, p85α, through dimerization with HER2, which lacks the appropriate bindings site(s) for p85α (31, 32). HER3 exhibited a high level of basal tyrosine phosphorylation and constitutive association with p85α and HER2 (or EGFR), which are abrogated by gefitinib (Fig. 3A; ref. 30). Similar results have been reported by Moulder et al. (33) with human breast cancer cell lines. Engelman et al. (34) reported that HER3 was associated with PI3K exclusively in gefitinib-sensitive NSCLC cell lines harboring either WT or mutant (L858R and del 747-749) EGFR. Gefitinib dissociated this complex and released p85α in gefitinib-sensitive cell lines. HER3 thus activates PI3K/Akt signaling through dimerization with either EGFR or HER2 molecule only in gefitinib-sensitive cancer cells (Fig. 3C).

Moreover, concomitant overexpression of both HER2 and HER3 was detected in two of eight lung cancer cell lines in culture, and these two cell lines were found to be highly susceptible to gefitinib (13), again suggesting the close association of HER2 and HER3 coexpression with gefitinib sensitivity (Fig. 4A). Moasser et al. (25) also reported that four human breast cancer cell lines overexpressing HER2 together with HER3 expression were more sensitive to gefitinib than the other cell lines examined (Fig. 4B). This close correlation of HER2 overexpression with gefitinib sensitivity therefore occurs in both lung (Fig. 4A) and breast cancer cells (Fig. 4B). Gefitinib inhibition of cell growth is possibly mediated through blockage of HER2/EGFR and/or HER3/EGFR heterodimer formation (26). HER2 expression is thus expected to play a pivotal role in the therapeutic efficacy not only of HER2 monoclonal antibodies (35) but also of EGFR tyrosine kinase inhibitors.

EGFR-targeting drugs could overcome accumulating resistance to trastuzumab in human breast cancer cells, plausibly through modulation of PI3K/Akt signaling (36). Because EGFR and other family members are often overexpressed in various other tumor types, the notion of how EGFR-targeting drugs show their therapeutic efficacies against lung and breast cancer would be applicable to the further development of such therapeutic strategies against other tumor types.

Other Molecular Determinants of Responses to Erlotinib, Cetuximab, and Gefitinib

Even with the notable responses conferred by EGFR inhibitors where there are activating mutations, the responses are not always durable, and there remain patients who do not have responses at all, so that additional strategies are needed to increase the effectiveness of EGFR-targeted therapy (12). Gefitinib is the first EGFR-targeting drug to be registered for advanced NSCLC followed by erlotinib, which possesses slightly different pharmacologic characteristics. On the other hand, cetuximab, a chimeric monoclonal antibody targeting EGFR, has been registered for the treatment of metastatic colorectal cancer (37). Mukohara et al. (38) have reported differential effects of gefitinib and cetuximab against NSCLC cells harboring activating EGFR mutations. Whereas activating mutations were associated with sensitivity to gefitinib but not to cetuximab, one particular deletion mutant, del E746-A750, was associated with sensitivity to cetuximab. However, little clinical experience has been gained in the use of cetuximab in advanced NSCLC and other malignancies. Other EGFR-targeting treatments, including monoclonal antibodies, small molecules, and vaccines, are now in clinical trials (39).

Combining EGFR-targeting drugs with anticancer agents could modify the characteristics of drug sensitivity in ways that might be unique for each drug type. Cooperative growth inhibition is often observed following a combination of EGFR-targeting drugs against various cancer cell types (40–43). Huang et al. (40) showed that combining cetuximab with either gefitinib or erlotinib synergistically enhanced growth inhibition in head/neck cancer cells and other tumor

types both *in vitro* and *in vivo* with a concomitant inhibition of EGFR phosphorylation. Furthermore, cetuximab resistance could be overcome by combination with erlotinib or gefitinib. The combination of cetuximab and erlotinib blocked erlotinib-induced EGFR up-regulation, resulting in apoptosis and growth inhibition of biliary tract cancer cells (42). Drug sensitivity and resistance could be regulated through common mechanisms among various EGFR-targeting drugs, such as protein expression levels, gene mutation, and gene gain of *EGFR*.

Van Schaeybroeck et al. (44) reported that EGFR activity contributes to colorectal cancer cell response to gefitinib alone and in combination with chemotherapeutic drugs. Colorectal cancer cell lines with high constitutive EGFR phosphorylation were found to be more sensitive to gefitinib than those with low EGFR phosphorylation. In addition, treatment with oxaliplatin or 5-fluorouracil increased EGFR phosphorylation; in those cell lines, a combination of treatment with gefitinib resulted in a synergistic effect on growth inhibition. This study strongly indicates EGFR phosphorylation levels in the absence or presence of chemotherapeutic agents as a plausible surrogate marker for therapeutic responses by EGFR-targeting drugs alone or in combination with chemotherapy.

Antiangiogenic Effect of Gefitinib through PI3K/Akt Pathway

EGF and TGF-α are themselves known to be angiogenic factors (45, 46), and they also up-regulate expression of potent angiogenic factors, vascular endothelial growth factor (VEGF) and interleukin-8, in cancer cells (47, 48). EGFR activation is often linked to angiogenesis as well as to invasion and metastasis, all processes thus able to be affected by EGFR antagonists (see Fig. 1). We investigated whether the antitumor effect of gefitinib was partly attributable to antiangiogenic activity. EGF markedly induced angiogenesis in an avascular area of the mouse cornea at similar levels to VEGF, and this EGF-induced neovascularization was almost completely blocked by gefitinib (Fig. 5A; ref. 47). Moreover, EGF-induced production of the angiogenic factors interleukin-8 and VEGF was almost completely blocked by gefitinib in cancer cells and was partially inhibited by SU5416, a selective inhibitor of VEGF receptor tyrosine kinases (Fig. 5B). We recently reported that the EGF/TGF-α–dependent up-regulation of angiogenic factors, such as VEGF and interleukin-8, is specifically mediated through PI3K/Akt activation rather than through ERK1/2 in cancer cells (48). Expression of EGFR was also reported in tumor-associated endothelial cells (49, 50) and endothelial cells of neovasculatures (51), suggesting that endothelial cells could be one of the targets for anticancer therapy by EGFR-targeting drugs. The antiangiogenic effects of gefitinib could be mediated directly by blocking EGF-induced neovascularization and also indirectly by inhibition of VEGF or interleukin-8 production.

Treatment with anti-VEGF monoclonal antibody bevacizumab (Avastin) in combination with anticancer agents provided the first clear demonstration of better survival outcomes over chemotherapy alone in patients with advanced colorectal cancers (52). VEGF and EGF exert their biological effects directly or indirectly on tumor growth and metastasis/invasion as well as on tumor angiogenesis. The biological effects by VEGF and EGF are mediated through activation of their specific downstream signalings, but both factors also share common downstream signaling pathways This is thus the potential for improved therapeutic efficacy by combination of both EGF/EGFR–targeting and VEGF/VEGF receptor–targeting drugs. Clinical trials of combinations of these molecular targeting drugs have been applied to lung cancer and other tumor types (53, 54). Herbst et al. (55) have evaluated bevacizumab in combination with erlotinib for NSCLC in a phase I/II trial and observed encouraging antitumor activity and safety, supporting further development of this combination (55). Furthermore, several clinical trials with VEGF receptor tyrosine kinase inhibitors are also now in progress (53–55). These VEGF receptor tyrosine kinase inhibitors, such as vatalanib (PTK787/ZK222584), semaxanib (SU5419), sorafenib (BAY439006), and zactima (ZD6474), can also inhibit the tyrosine kinase activities of EGFR, platelet-derived growth factor receptor, c-Kit, Raf, and Flt-3; these drugs are thus considered multitargeted tyrosine kinase inhibitors. Of these multitargeted drugs, ZD6474, for example, has a potent inhibitory activity not only on VEGF receptor-2 tyrosine kinase of vascular endothelial cells but also on EGFR tyrosine kinase of cancer cells, resulting in the suppression of tumor angiogenesis, tumor growth, and invasion/metastasis. Whether the multitargeted therapeutic approach or the combination of selective targeting agents will have better therapeutic efficacy against each human tumor type is a matter of debate.

Conclusion

In preclinical studies, HER2 and/or HER3 expression can sensitize cancer cells to gefitinib. Moreover, Akt activation following HER2/HER3 heterodimer formation seems to play a pivotal role in the sensitivity to EGFR-targeting drugs. EGFR-targeting drug sensitivity is largely dependent on the extent to which Akt or STAT activation as well as ERK1/2 activation is associated with EGFR-induced cell survival and cell growth in each cancer. Gene mutations, gene gains, and expression levels lead to EGFR activation without ligand binding, resulting in altered sensitivity to EGFR-targeting drugs. To predict the therapeutic efficacies of gefitinib and other EGFR-targeting drugs, standard assay systems, such as immunohistochemistry and fluorescence *in situ* hybridization, are required to evaluate *EGFR* mutations, gene gain, and protein expression levels. We expect that the combination of various tyrosine kinase inhibitors or multitargeted inhibitors might have better therapeutic benefits.

Acknowledgments

We thank our colleagues N. Shinbaru, A. Hirata, S. Ueda, and F. Hosoi at Kyushu University (Fukuoka, Japan) for their collaboration in this study.

References

1. Lemmon MA, Schlessinger J. Regulation of signal transduction and signal diversity by receptor oligomerization. Trends Biochem Sci 1994;19:459–63.
2. Sirotnak FM, Zakowski MF, Miller VA, Scher HI, Kris MG. Efficacy of cytotoxic agents against human tumor xenografts is markedly enhanced by coadministration of ZD1839 (Iressa), an inhibitor of EGFR tyrosine kinase. Clin Cancer Res 2000;6:4885–92.
3. Arteaga CL. Epidermal growth factor receptor dependence in human tumors: more than just expression? Oncologist 2002;4:31–9.
4. Reinmuth N, Meister M, Muley T, et al. Molecular determinants of response to RTK-targeting agents in nonsmall cell lung cancer. Int J Cancer 2006;119:727–34.
5. Brabender J, Danenberg KD, Metzger R, et al. Epidermal growth factor receptor and HER2-*neu* mRNA expression in non-small cell lung cancer is correlated with survival. Clin Cancer Res 2001;7:1850–5.
6. Cappuzzo F, Hirsch FR, Rossi E, et al. Epidermal growth factor receptor gene and protein and gefitinib sensitivity in non-small-cell lung cancer. J Natl Cancer Inst 2005;97:643–55.
7. Lynch TJ, Bell DW, Sordella R, et al. Activating mutations in the epidermal growth factor receptor underlying responsiveness of non-small-cell lung cancer to gefitinib. N Engl J Med 2004;350:2129–39.
8. Paez JG, Janne PA, Lee JC, et al. EGFR mutations in lung cancer: correlation with clinical response to gefitinib therapy. Science 2004;304:1497–500.
9. Pao W, Miller V, Zakowski M, et al. EGF receptor gene mutations are common in lung cancers from "never smokers" and are associated with sensitivity of tumors to gefitinib and erlotinib. Proc Natl Acad Sci U S A 2004;101:13306–11.
10. Taron M, Ichinose Y, Rosell R, et al. Activating mutations in the tyrosine kinase domain of the epidermal growth factor receptor are associated with improved survival in gefitinib-treated chemorefractory lung adenocarcinomas. Clin Cancer Res 2005;11:5878–85.
11. Bates SE, Fojo T. Epidermal growth factor receptor inhibitors: a moving target? Clin Cancer Res 2005;11:7203–5.
12. Tsao MS, Sakurada A, Cutz JC, et al. Erlotinib in lung cancer-molecular and clinical predictors of outcome. N Engl J Med 2005;353:133–44.
13. Ono M, Hirata A, Kometani T, et al. Sensitivity to gefitinib (Iressa, ZD1839) in non-small cell lung cancer cell lines correlates with dependence on the epidermal growth factor (EGF) receptor/extracellular signal-regulated kinase 1/2 and EGF receptor/Akt pathway for proliferation. Mol Cancer Ther 2004;3:465–72.
14. Sodella R, Bell DW, Haber DA, Settleman J. Gefitinib-sensitizing EGFR mutations in lung cancer activate anti-apoptotic pathways. Science 2004;305:1163–7.
15. Cappuzzo F, Magrini E, Ceresoli GL, et al. Akt phosphorylation and gefitinib efficacy in patients with advanced non-small-cell lung cancer. J Natl Cancer Inst 2004;96:1133–41.
16. Pao W, miller VA, Venkatraman E, Kris MG. Predicting sensitivity of non-small-cell lung cancer to gefitinib: is there a role for P-Akt? J Natl Cancer Inst 2004;96:1117–9.
17. Riely G, Pao W, Pham D, et al. Clinical course of patients with non-small cell lung cancer and epidermal growth factor receptor exon 19 and exon 21 mutations treated with gefitinib or erlotinib. Clin Cancer Res 2006;12:839–44.
18. Jänne PA, Johnson BE. Effect of epidermal growth factor receptor tyrosine kinase domain mutations on the outcome of patients with non-small cell lung cancer treated with epidermal growth factor receptor tyrosine kinase inhibitors. Clin Cancer Res 2006;12:4416–20.
19. Mitsudomi T, Viallet J, Mulshine JL, Linnoila RI, Minna JD, Gazdar AF. Mutations of ras genes distinguish a subset of non-small-cell lung cancer cell lines from small-cell lung cancer cell lines. Oncogene 1991;6:1353–62.
20. Pao W, Wang TY, Riely GJ, et al. KRAS mutations and primary resistance of lung adenocarcinomas to gefitinib or erlotinib. PLoS Med 2005;2:57–61.
21. Kosaka T, Yatabe Y, Endoh H, Kuwano H, Takahashi T, Mitsudomi T. Mutations of epidermal growth factor receptor gene in lung cancer: biological and clinical implications. Cancer Res 2004;64:8919–23.
22. Hirsch FR, Varella-Garcia M, McCoy J, et al. Increased epidermal growth factor receptor gene copy number detected by fluorescence *in situ* hybridization associates with increased sensitivity to gefitinib in patients with bronchioloalveolar carcinoma subtypes: a Southwest Oncology Group Study. J Clin Oncol 2005;23:6838–45.
23. Takano T, Ohe Y, Sakamoto H, et al. Epidermal growth factor receptor gene mutations and increased copy numbers predict gefitinib sensitivity in patients with recurrent non-small-cell lung cancer. J Clin Oncol 2005;1:6829–37.
24. Slamon DJ, Clark GM, Wong SG, Levin WJ, Ullrich A, McGuire WL. Human breast cancer: correlation of relapse and survival with amplification of the HER-2/*neu* oncogene. Science 1987;235:177–82.
25. Moasser MM, Basso A, Averbuch SD, Rosen N. The tyrosine kinase inhibitor ZD1839 ("Iressa") inhibits HER2-driven signaling and suppresses the growth of HER2-overexpressing tumor cells. Cancer Res 2001;61:7184–8.
26. Anido J, Matar P, Albanell J, et al. ZD1839, a specific epidermal growth factor receptor (EGFR) tyrosine kinase inhibitor, induces the formation of inactive EGFR/HER2 and EGFR/HER3 heterodimers and prevents heregulin signaling in HER2-overexpressing breast cancer cells. Clin Cancer Res 2003;9:1274–83.
27. Cappuzzo F, Varella-Garcia M, Shigematsu H, et al. Increased HER2 gene copy number is associated with response to gefitinib therapy in epidermal growth factor receptor-positive non-small-cell lung cancer patients. J Clin Oncol 2005;1:5007–18.
28. Shigematsu H, Takahashi T, Nomura M, et al. Somatic mutations of the HER2 kinase domain in lung adenocarcinomas. Cancer Res 2005;65:1642–6.
29. Cappuzzo F, Bemis L, Varella-Garcia M. HER2 mutation and response to trastuzumab therapy in non-small-cell lung cancer. N Engl J Med 2006;354:2619–21.
30. Hirata A, Hosoi F, Miyagawa M, et al. HER2 overexpression increases sensitivity to gefitinib, an epidermal growth factor receptor tyrosine kinase inhibitor, through inhibition of HER2/HER3 heterodimer formation in lung cancer cells. Cancer Res 2005;65:4253–60.
31. Prigent SA, Gullick WJ. Identification of c-erbB-3 binding sites for phosphatidylinositol 3′-kinase and SHC using an EGF receptor/c-erbB-3 chimera. EMBO J 1994;13:2831–41.
32. Soltoff SP, Carraway KL III, Prigent SA, Gullick WG, Cantley LC. ErbB3 is involved in activation of phosphatidylinositol 3-kinase by epidermal growth factor. Mol Cell Biol 1994;14:3550–8.
33. Moulder SL, Yakes FM, Muthuswamy SK, Bianco R, Simpson JF, Arteaga CL. Epidermal growth factor receptor (HER1) tyrosine kinase inhibitor ZD1839 (Iressa) inhibits HER2/*neu* (erbB2)-overexpressing breast cancer cells *in vitro* and *in vivo*. Cancer Res 2001;61:8887–95.
34. Engelman JA, Janne PA, Mermel C, et al. ErbB-3 mediates phosphoinositide 3-kinase activity in gefitinib-sensitive non-small cell lung cancer cell lines. Proc Natl Acad Sci U S A 2005;102:3788–93.
35. Yarden Y. Biology of HER2 and its importance in breast cancer. Oncology 2001;61 Suppl 2:1–13.
36. Chan CT, Metz MZ, Kane SE. Differential sensitivities of trastuzumab (Herceptin)-resistant human breast cancer cells to phosphoinositide-3 kinase (PI-3K) and epidermal growth factor receptor (EGFR) kinase inhibitors. Breast Cancer Res Treat 2005;91:187–201.
37. Cunningham D, Humblet Y, Siena S, et al. Cetuximab monotherapy and cetuximab plus irinotecan in irinotecan-refractory metastatic colorectal cancer. N Engl J Med 2004;351:337–45.
38. Mukohara T, Engelman JA, Hanna NH, et al. Differential effects of gefitinib and cetuximab on non-small-cell lung cancers bearing epidermal growth factor receptor mutations. J Natl Cancer Inst 2005;97:1185–94.
39. Giaccone G. Epidermal growth factor receptor inhibitors in the treatment of non-small-cell lung cancer. J Clin Oncol 2005;23:3235–42.
40. Huang S, Armstrong EA, Benavente S, et al. Dual-agent molecular targeting of the epidermal growth factor receptor (EGFR): combining anti-EGFR antibody with tyrosine kinase inhibitor. Cancer Res 2004;64:5355–62.
41. Huether A, Hopfner M, Baradari V, et al. EGFR blockade by cetuximab alone or as combination therapy for growth control of hepatocellular cancer. Biochem Pharmacol 2005;70:1568–78.
42. Jimeno A, Rubio-Viqueira B, Amador ML, et al. Epidermal growth factor receptor dynamics influences response to epidermal growth factor receptor targeted agents. Cancer Res 2005;65:3003–10.
43. Nakamura H, Takamori S, Fujii T, et al. Cooperative cell-growth inhibition by combination treatment with ZD1839 (Iressa) and trastuzumab (Herceptin) in non-small-cell lung cancer. Cancer Lett 2005;230:33–46.
44. Van Schaeybroeck S, Karaiskou-Mc Caul A, Kelly D, et al. Epidermal growth factor receptor activity determines response of colorectal cancer cells to gefitinib alone and in combination with chemotherapy. Clin Cancer Res 2005;11:7480–9.
45. Schreiber AB, Winkler ME, Derynck R. Transforming growth factor-α: a more potent angiogenic mediator than epidermal growth factor. Science 1986;232:1250–3.
46. Gospodarowicz D, Bialecki H. Fibroblast and epidermal growth factors are mitogenic agents for cultured granulosa cells of rodent, porcine, and human origin. Endocrinology 1979;104:757–64.
47. Hirata A, Ogawa S, Kometani T, et al. ZD1839 (Iressa) induces antiangiogenic effects through inhibition of epidermal growth factor receptor tyrosine kinase. Cancer Res 2002;62:2554–60.
48. Ueda S, Basaki Y, Yoshie M, et al. PTEN/Akt signaling through epidermal growth factor receptor is prerequisite for angiogenesis by hepatocellular carcinoma cells that is susceptible to inhibition by gefitinib. Cancer Res 2006;66:5346–53.
49. Baker CH, Kedar D, McCarty MF, et al. Blockade of epidermal growth factor receptor signaling on tumor cells and tumor-associated endothelial cells for therapy of human carcinomas. Am J Pathol 2002;161:929–38.
50. Kim SJ, Uehara H, Karashima T, Shepherd DL,

Killion JJ, Fidler IJ. Blockade of epidermal growth factor receptor signaling in tumor cells and tumor-associated endothelial cells for therapy of androgen-independent human prostate cancer growing in the bone of nude mice. Clin Cancer Res 2003; 9:1200–10.

51. Hirata A, Uehara H, Izumi K, Naito S, Kuwano M, Ono M. Direct inhibition of EGF receptor activation in vascular endothelial cells by gefitinib ('Iressa', ZD1839). Cancer Sci 2004;95:614–8.
52. Hurwits H, Fehrenbacher L, Novotny W, et al. Bevacizumab plus irinotecan, fluorouracil, and leucovorin for metastatic colorectal cancer. N Engl J Med 2004; 350:2335–42.
53. Maione P, Gridelli C, Troiani T, Ciardiello F. Combination targeted therapies and drugs with multiple targets in the treatment of NSCLC. Oncologist 2006;11:274–84.
54. Morabito A, Maio ED, Maio MD, Normanno N, Perrone F. Tyrosine kinase inhibitors of vascular endothelial growth factor receptors in clinical trials: current status and future directions. Oncologist 2006;11: 753–64.
55. Herbst RS, Johnson DH, Mininberg E, et al. Phase I/II trial evaluating the anti-vascular endothelial growth factor monoclonal antibody bevacizumab in combination with the HER-1/epidermal growth factor receptor tyrosine kinase inhibitor erlotinib for patients with recurrent non-small-cell lung cancer. J Clin Oncol 2005;12:2544–55.

Liver International 2006; 26: 964–975

Liver International
DOI: 10.1111/j.1478-3231.2006.01321.x

Clinical Studies

Growth inhibitory effects of pegylated IFN α-2b on human liver cancer cells *in vitro* and *in vivo*

Yano H, Ogasawara S, Momosaki S, Akiba J, Kojiro S, Fukahori S, Ishizaki H, Kuratomi K, Basaki Y, Oie S, Kuwano M, Kojiro M. Growth inhibitory effects of pegylated IFN α-2b on human liver cancer cells *in vitro* and *in vivo*. Liver International 2006: 26: 964–975

Abstract: *Purpose:* We investigated the effects of pegylated IFN-α2b (PEG-IFN-α2b) on the growth of human liver cancer cells. *Methods:* The effect of PEG-IFN-α2b on the proliferation of 13 liver cancer cell lines was investigated *in vitro*. Chronological changes in growth and IFN-α receptor-2 (IFNAR-2) expression were monitored in hepatocellular carcinoma (HCC) cells (HAK-1B) cultured with PEG-IFN-α2b. After HAK-1B cells were transplanted into nude mice, various doses of PEG-IFN-α2b or IFN-α2b were administered, and tumor volume, weight, histology, and IFNAR-2 expression were examined. *Results:* PEG-IFN-α2b inhibited the growth of nine cell lines with apoptosis in a dose- and time-dependent manner. Continuous contact with PEG-IFN-α2b induced time-dependent growth inhibition and down-regulation of IFNAR-2 expression. PEG-IFN-α2b induced a dose-dependent decrease in tumor volume and weight, a significant increase of apoptotic cells, and a decrease in IFNAR-2 expression in the tumor. The clinical dose for chronic hepatitis C was also effective. The antitumor effect of PEG-IFN-α2b was significantly stronger than that of non-PEG-IFN-α2b *in vivo*. *Conclusions:* Continuous contact with PEG-IFN-α2b induces strong antitumor effects and the down-regulation of IFNAR-2 in HCC cells. The data suggest potential clinical application of PEG-IFN-α2b for the prevention and treatment of HCC.

Hirohisa Yano[1,2], Sachiko Ogasawara[1,2], Seiya Momosaki[1,2], Jun Akiba[1,2], Sakiko Kojiro[1,2], Suguru Fukahori[1,2], Hironori Ishizaki[1,2], Keitaro Kuratomi[1,2], Yuji Basaki[3], Shinji Oie[3], Michihiko Kuwano[2,4] and Masamichi Kojiro[1,2]

[1]Department of Pathology, Kurume University School of Medicine, Kurume, Japan, [2]Research Center of Innovative Cancer Therapy of the 21st Century COE Program for Medical Science, Kurume University, Kurume, Japan, [3]Station-II for Collaborative Research, Kyushu University, Fukuoka, Japan, [4]Research Center of Innovative Cancer Therapy, Kurume University, Kurume, Japan

Key words: apoptosis – hepatocellular carcinoma – nude mouse – pegylated interferon – receptor

Hirohisa Yano, MD, Department of Pathology, Kurume University School of Medicine 67 Asahi-machi, Kurume, Fukuoka 830-0011, Japan.
Tel: +81 9 4231 7546
Fax: +81 9 4232 0905
e-mail: hiroyano@med.kurume-u.ac.jp

Received 17 March 2006,
accepted 17 May 2006

Interferon-α (IFN-α) is a multifunctional cytokine that possesses antiviral activity, antiproliferative activity, various immunoregulatory activities, antitelomerase activity, and antiangiogenesis activity (1–3). The antiviral activity of IFN-α has attracted much attention, and IFN-α preparations have been used in the treatment of hepatitis B virus- and hepatitis C virus (HCV)-related chronic hepatitis in many countries (4). Recently, IFN-α has been shown to possess highly suppressive effects on hepatocellular carcinogenesis and the recurrence of hepatocellular carcinoma (HCC) after curative treatment for HCC in patients with virus-related chronic hepatitis (5–10). However, the mechanisms of these actions have not yet been clarified. We previously reported that human lymphoblastoid IFN-α derived from Sendai virus-induced BALL-1 cells (BALL-1 IFN-α) directly suppressed the cell proliferation of 13 liver cancer cell lines to various degrees by inhibiting cell cycle progression with or without apoptosis *in vitro* (11). Recently, we also showed that consensus IFN-α at or close to the clinical dose used in treatment for HCV-related chronic hepatitis suppressed HCC growth in nude mice (12). This suggests that the direct antiproliferative action of IFN-α may be involved in the suppressive mechanisms of IFN-α on hepatocellular carcinogenesis. In clinical practice, IFN-α alone or in combination with other anticancer drugs such as 5-fluorouracil has been used in the treatment of malignant diseases including leukemia, renal cancer (4, 13) and advanced HCC (14).

Pegylated IFN α-2b (PEG-IFN-α2b) is a covalent conjugate of recombinant IFN-α2b with a monomethoxy polyethylene glycol (PEG) in a 1:1 molar ratio that produces a 31 000-Da molecule (15). PEG conjugation increases the size of the molecule. Therefore, the absorption of the pegylated molecule is slower, its serum half-life is longer, and its rate of clearance from the plasma is lower than that of the unmodified molecule. PEG-IFN-α2b thereby increases patient exposure to IFN-α2b and requires less frequent administration (15). Clinical trials in patients with chronic hepatitis C suggest that PEG-IFN-α preparations produce more potent therapeutic effects with or without ribavirin than do non-PEG-IFN-α preparations (15–20). However, whether or not PEG-IFN preparations are superior to non-PEG-IFN preparations in terms of suppressive effects on hepatocellular carcinogenesis and HCC growth has not been clarified. In addition, there have been no basic *in vitro* or *in vivo* studies that evaluate the efficacy of PEG-IFN-α2b on HCC cells. In the current study, we examined the *in vitro* and *in vivo* antitumor effects of PEG- and non-PEG-IFN-α2b on liver cancer cell lines by using several PEG-IFN-α2b concentrations including a low dose that is close to the clinical dose. We also examined the expression of type I IFN receptor 2 (IFNAR-2) subunit and its relationship with antitumor effects on HCC cells under the condition of continuous contact with PEG-IFN-α2b.

Materials and methods

Cell lines and cell culture

This study used 11 HCC cell lines (KIM-1, KYN-1, KYN-2, KYN-3, HAK-1A, HAK-1B, HAK-2, HAK-3, HAK-4, HAK-5, and HAK-6) and two human combined hepatocellular and cholangiocarcinoma (CHC) cell lines (KMCH-1 and KMCH-2). These HCC and CHC cell lines were originally established in our laboratory, and each cell line retains the morphological and functional features of the original tumor as described elsewhere (11, 21–29).

The cells were grown in Dulbecco's Modified Eagle Medium (Nissui Seiyaku Co., Tokyo, Japan) supplemented with 2.5% heat-inactivated (56 °C, 30 min) fetal bovine serum (FBS, Bioserum, Vic, Australia), 100 U/ml penicillin, 100 μg/ml streptomycin (GIBCO BRL/Life Technologies Inc., Gaithersburg, MD) and 12 mmol/l sodium bicarbonate, in a humidified atmosphere of 5% CO_2 in air at 37 °C.

IFN and reagents

PEG-IFN-α2b (PEG Intron®) and IFN-α2b (Intron®A) were kindly provided by Schering-Plough K.K. (Osaka, Japan). The specific activity of PEG-IFN-α2b was 6.4×10^7 IU/mg protein and that of IFN-α2b was 2.6×10^8 IU/mg protein.

Anti-bromodeoxyuridine (BrdU) antibody and fluorescein isothiocyanate-conjugated goat anti-mouse immunoglobulin (FITC-GAM) were purchased from BD Biosciences (San Jose, CA); control normal mouse IgG_1, from DAKO (Glostrup, Denmark); rat antibody against mouse endothelial cells (anti-CD34, clone MEC14.7), from Serotec Co., Oxford, UK; mouse monoclonal antibody against human α-smooth muscle actin (SMA) that cross-reacts with mouse α-SMA (clone 1A4), from Immunon (Pittsburgh, PA); rabbit antibody against vimentin fragment (V1) (caspase-9 activation state antibody (30)), from Medical & Biological Laboratories Co. Ltd. (Nagoya, Japan); mouse monoclonal antibody against human IFN α/β receptor chain 2, from Chemicon International Inc. (Temecula, CA); and mouse monoclonal antibody against human epidermal growth factor (EGF) receptor, from Upstate Biotechnology Incorporated (Lake Placid, NY).

Effects of PEG-IFN-α2b and IFN-α2b on the proliferation of HCC and CHC cell lines *in vitro*

The effects of PEG-IFN-α2b on the growth of the cultured cells were examined with colorimetry using 3-(4,5-dimethylthiazol-2yl)-2,5-diphenyl tetrazolium bromide (MTT) assay kits (Chemicon International Inc.) as described elsewhere (11, 12). Briefly, the cells ($1.5–8 \times 10^3$ cells per well) were seeded on 96-well plates (Nunc Inc., Roskilde, Denmark), cultured for 24 h, and the culture medium was changed to a new medium with or without PEG-IFN-α2b (16, 64, 256, 1024, or 4096 IU/ml). After culturing for 24, 48, 72 or 96 h, the number of viable cells was measured with ImmunoMini NJ-2300 (Nalge Nunc International, Tokyo, Japan) by setting the test wavelength at 570 nm and the reference wavelength at 630 nm. To keep the optical density within linear range, all experiments were performed while the cells were in the logarithmic growth phase. The effects of IFN-α2b on the growth of the cell lines were also examined in the same manner.

Morphological observation

For morphological observation under a light microscope, cultured cells were seeded on Lab-

Tek tissue culture chamber slides (Nunc Inc.), cultured with or without PEG-IFN-α2b (256, 1024 or 4096 IU/ml) for 72 h, fixed for 10 min in Carnoy's solution, and stained with hematoxylin–eosin (HE).

Quantitative analysis of PEG-IFN-α2b-induced apoptosis *in vitro*

The cells cultured with or without 1000 IU/ml PEG-IFN-α2b for 72 h were stained with the Annexin V-EGFP (enhanced green fluorescent protein) Apoptosis Detection Kits (Medical & Biological Laboratories Co., Ltd.) according to the manufacturer's protocol. After staining, the cells were analyzed using a FACScan (Becton Dickinson Immunocytometry Systems, San Jose, CA), and Annexin V-EGFP-positive apoptotic cell rate was determined.

Effects of PEG-IFN-α2b on the proliferation and expression of the IFNAR-2 subunit

To investigate the expression of the IFNAR-2 subunit after continuous contact of PEG-IFN-α2b as well as its relationship with antiproliferative effects, HAK-1B cells were cultured with medium alone (Control) or medium containing 1000 IU/ml of PEG-IFN-α2b for 0, 3, 24, 48, 72, 96, 144, 192 or 240 h. The viable cell number and the cell surface expression of the IFNAR-2 subunit were examined. The cell surface expression of the IFNAR-2 subunit was analyzed using flow cytometry with the technique described elsewhere (11) with slight modification. Briefly, the cells were reacted with anti-IFN α/β receptor chain 2 antibody (final concentration, 2.5 μg/ml) or control antibody for 1 h, washed once, incubated with 4 μl of FITC-GAM for 30 min, washed once, fixed in 4% paraformaldehyde for 10 min, washed, and analyzed with a FACScan. The expression levels were compared according to the mean channel number. As an internal control to confirm that cell surface protein level on HAK-1B cells treated with or without 1000 IU/ml of PEG-IFN-α2b is constant, EGF receptor expression was measured on the cells cultured for 240 h in the same manner. After culturing for 72 h, cell cycle analysis was also performed in HAK-1B cells cultured with or without 1000 IU/ml of PEG-IFN-α2b with the technique described elsewhere (11). Briefly, cells were labeled with 10 mM BrdU (Sigma Chemical Co., St Louis, MO) for 30 min, harvested, fixed in 70% cold ethanol at 4 °C overnight, stained with anti-BrdU and propidium iodide (Sigma Chemical Co.), and analyzed by using a FACScan.

Effects of PEG-IFN-α2b and IFN-α2b on HCC cell proliferation in nude mice

Cultured HAK-1B (10^7 cells/mouse) was subcutaneously (sc) injected into the backs of 5-week-old female BALB/c athymic nude mice (Clea Japan Inc., Osaka, Japan). Five to seven days later when the largest diameter of the tumor reached approximately 5–10 mm (Day 0), the mice were divided into seven groups ($n = 6$–9 each) in the first experiment (Experiment #1) and into five groups ($n = 7$ or 8 each) in the second experiment (Experiment #2) in a manner to equalize the mean tumor diameter of every group. In Experiment #1, each mouse received a sc injection of 0.1 ml of medium alone (Control), medium containing 640, 6400, 64 000, or 640 000 IU of PEG-IFN-α2b, or medium containing 6400 or 64 000 IU of IFN-α2b, twice a week for two consecutive weeks (Day 1, Day 4, Day 8, and Day 11). Experiment #2 was conducted in the same manner but 640 and 6400 IU/mouse of PEG-IFN-α2b and the same doses of IFN-α2b were used. The aim of Experiment #2 was to examine the reproducibility of the antitumor effects of PEG-IFN-α2b at low concentrations and to compare this activity to that of IFN-α2b. The clinical dose of PEG-IFN-α2b in chronic hepatitis C treatment is 9.6×10^4 IU/kg and is three times the lowest dose (3.2×10^4 IU/kg) in the experiment. During this 2-week period, tumor size was measured in two directions using calipers on the first and second days of sc injection (Day 1 and Day 2) and then once every 2 days until Day 14, and tumor volume (mm^3) was estimated using the equation 'length × $(\text{width})^2 \times 0.5$'. Mouse body weight was measured on Day 0, Day 8, and Day 14. On Day 15, the mice were sacrificed and the tumors were resected and weighed and used for morphological studies (e.g., HE staining and immunohistochemistry) and ELISA analysis. Every mouse received an intraperitoneal injection of 1 mg of BrdU 30 min before sacrifice.

The animals received human care according to the criteria outlined in the 'Guide for the Care and Use of Laboratory Animals' prepared by the National Academy of Sciences and published by the National Institutes of Health (NIH publication 86-23 revised 1985).

Morphological examination of the subcutaneous tumors of nude mice

The number of cells showing the characteristics of apoptosis (e.g., cytoplasmic shrinkage, chromatin condensation, and nuclear fragmentation) was counted in ten 0.25 mm^2 areas within an HE-stained specimen of the first experiment, and the

average number per area was obtained. The appearance of apoptotic cells was confirmed by the immunohistochemical detection of vimentin fragment (V1), i.e., a marker for caspase-9 activation (30), with the specific antibody and HistoMouse™-plus kits (Zymed Laboratories Inc., CA). The specimens were also immunostained for incorporated BrdU using BrdU Staining Kits (Oncogene Research Products, Boston, MA), and the average number of positive cells per area was obtained as described above. In addition, double-immunostaining was performed with anti-mouse endothelial cell antibody, anti-human α-SMA antibody, Histofine simple stain mouse MAX-PO (Rat) kits (Nichirei, Tokyo, Japan), and HistoMouse™-plus kits to detect artery-like blood vessels as described in our previous report (12, 31). The number of blood vessels in the tumor nodule was counted on each specimen. The size of the counted area was traced and measured using TurboCAD software (IMSI, Novato, CA). From the number of vessels per unit area (mm^2) obtained, the group mean was obtained for group comparison.

ELISA

The tumors were cut into pieces, and an appropriate amount was homogenized in 500 µl of ice-cold Ca^{2+}- and Mg^{2+}-free phosphate-buffered saline containing 100 µg/ml phenymethylsulfonyl fluoride using a pellet pestle. The mixture was centrifuged for 10 min (12 000 g, 4 °C), and the supernatant was stored at −20 °C until use. The amount of the IFNAR-2 subunit in the supernatant was measured using ELISA kits (Otsuka Pharmaceutical Co. Ltd., Tokyo, Japan). The amount of tissue protein was determined using a BCA protein assay reagent (Pierce, Rockford, IL).

Statistics

Comparisons of estimated tumor volume and colorimetric cell growth were performed using two-factor factorial ANOVA and Student's *t*-test, respectively. The other data comparisons were performed using the Mann–Whitney *U*-test.

Results

Effects of PEG-IFN-α2b on liver cancer cell proliferation *in vitro*

Twenty-four hours after the addition of 4096 IU/ml of PEG-IFN-α2b, mild increase in the relative viable cell number occurred in 10 cell lines (all cell lines except HAK-1B, HAK-6, and KMCH-1). However, after 72 h or later, a 10% or more decrease in the cell number occurred in 12 cell lines (Fig. 1A). In HAK-3, proliferation was not suppressed but slightly promoted up to 96 h of PEG-IFN-α2b contact. In HAK-2 and HAK-4, proliferation was suppressed up to 72 h and the cell number reached a plateau thereafter. In the other 10 cell lines, proliferation was suppressed to varying degrees up to 96 h.

Ninety-six hours after the addition of PEG-IFN-α2b, the relative viable cell number was suppressed in nine cell lines (all cell lines except HAK-2, HAK-3, HAK-4, and KMCH-2) in a dose-dependent manner (Fig. 1B). In four cell lines (KYN-2, HAK-1B, KYN-1, and KIM-1), the number was suppressed to 50% or less with 4096 IU/ml of PEG-IFN-α2b, and the 50% inhibitory concentration (IC50) was 831.8 IU/ml for KYN-2, 839.0 IU/ml for HAK-1B, 1298.6 IU/ml for KYN-1, and 3396.4 IU/ml for KIM-1. The IC50 of non-PEG-IFN-α2b in the four cell lines was 918.5, 627.7, 1237.7, and 2617.8 IU/ml, respectively, which was not significantly different from that of PEG-IFN-α2b (paired Student's *t*-test). No relationship was detected between the histological differentiation level of the original tumor and sensitivity to the antiproliferative effect of PEG-IFN-α2b.

Seventy-two hours after adding 4096 IU/ml of PEG-IFN-α2b, 10 cell lines (all cell lines except HAK-2, HAK-3, and KMCH-2) presented characteristics of apoptosis, e.g., cytoplasmic shrinkage, chromatin condensation, and nuclear fragmentation, to various degrees (Fig. 2).

Quantitative analysis of Annexin V-EGFP-positive apoptotic cells revealed that the appearance of apoptosis was significantly higher in the cultures with 1000 IU/ml of PEG-IFN-α2b than those without PEG-IFN-α2b in nine cell lines (Table 1).

Effects of PEG-IFN-α2b on the proliferation and expression of IFNAR-2 *in vitro*

With continuous contact of PEG-IFN-α2b up to 240 h, the expression of IFNAR-2 in HAK-1B cells was significantly down-regulated at 3 h compared with the Control, then significantly up-regulated at 48 h, and significantly down-regulated in the period between 96 and 240 h (Fig. 3A). To check the specificity of the down-regulation of IFNAR-2 expression, the expression of EGF receptor was also analyzed at 240 h. The mean channel numbers of HAK-1B cells cultured with and without 1000 IU/ml of PEG-IFN-α2b were 10.1 ± 0.4 and 10.6 ± 0.9, respectively, and there was no significant difference in EGF recep-

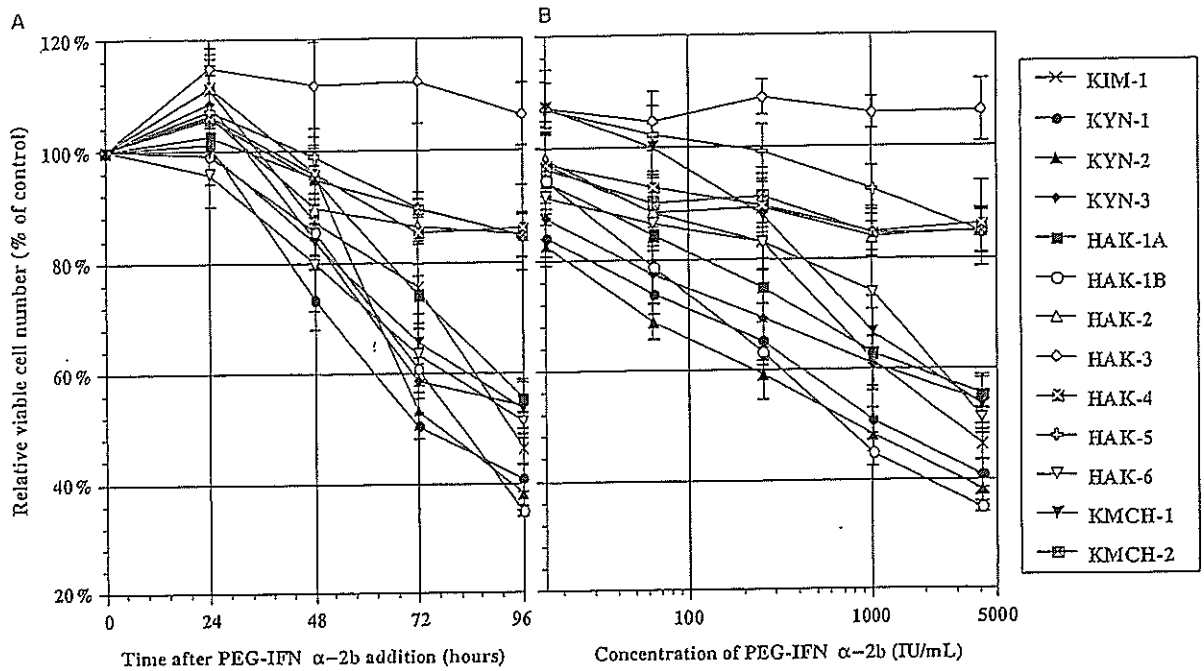

Fig. 1. Antiproliferative effect of pegylated IFN-α2b (PEG-IFN-α2b). (A) Chronological changes in relative viable cell number (% of the control) after adding 4096 IU/ml of PEG-IFN-α2b. Growth was suppressed with time in 10 cell lines. (B) 96 h after adding 16, 64, 256, 1024, or 4096 IU/ml of PEG-IFN-α2b. Cell proliferation was suppressed in a dose-dependent manner in nine cell lines. The suppression was significant ($P<0.001$–0.05) in the ranges of 16–4096 IU/ml of PEG-IFN-α2b in KYN-1, KYN-2, and HAK-6; 64–4096 IU/ml in KYN-3, HAK-1A, HAK-1B, and HAK-2; 256–4096 IU/ml in KIM-1 and KMCH-1; 1024–4096 IU/ml in KMCH-2; and at 4096 IU/ml in HAK-5 (Student's *t*-test). Eight samples were used in each experiment ($n = 8$). The experiment was repeated at least three times for each cell line. The figures represent average ± SE of the experiments.

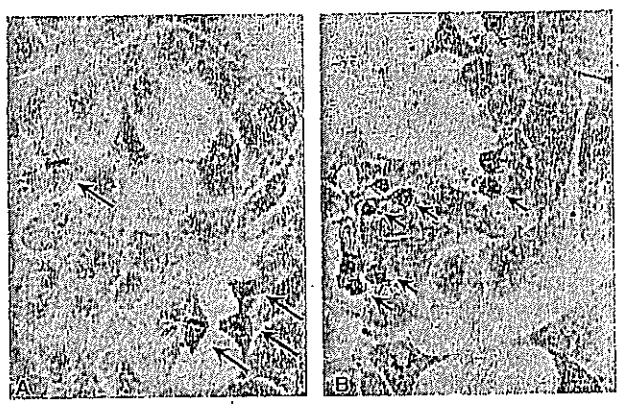

Fig. 2. Photomicrograph of HAK-1B cells cultured for 72 h on a Lab-Tek Chamber slide, (A) Without pegylated IFN-α2b (PEG-IFN-α2b) in culture medium. Some mitotic figures (long arrows) were noted. (B) With 4096 IU/ml of PEG-IFN-α2b in culture medium. Apoptotic cells (short arrows) characterized by cytoplasmic shrinkage, chromatic condensation and nuclear fragmentation were noted (hematoxylin–eosin staining, ×200).

Table 1. Quantitative analysis of apoptosis induced by PEG-IFN-α2b in 13 liver cancer cell lines

	Annexin V-EGFP-positive apoptotic cells (%)	
Cell line	Control	PEG-IFN-α2b
KIM-1	5.9 ± 0.2	28.0 ± 0.7†
KYN-1	4.7 ± 1.0	6.6 ± 0.5
KYN-2	0.6 ± 0.1	3.1 ± 0.7†
KYN-3	14.2 ± 2.4	21.5 ± 1.0*
HAK-1A	8.6 ± 0.3	14.8 ± 0.4†
HAK-1B	5.4 ± 0.4	25.0 ± 0.5†
HAK-2	0.5 ± 0.1	0.2 ± 0.0
HAK-3	3.2 ± 0.4	4.7 ± 0.6
HAK-4	4.6 ± 1.0	9.2 ± 0.3†
HAK-5	5.8 ± 0.1	9.1 ± 0.3†
HAK-6	13.6 ± 0.7	31.4 ± 0.4†
KMCH-1	2.9 ± 0.1	15.8 ± 0.5†
KMCH-2	5.3 ± 0.4	3.6 ± 0.6

Cells were cultured with medium alone (Control) or medium with 1000 IU/ml of PEG-IFN-α2b. Apoptosis was measured by Annexin V-EGFP staining. The rates of Annexin V-EGFP-positive apoptotic cell were shown as average ± SE. Five samples were used in each experiment. *$P<0.05$, vs corresponding control value. †$P<0.01$, vs corresponding control value. PEG-IFN-α2b, pegylated IFN-α2b; EGFP, enhanced green fluorescent protein.

tor expression. The relative viable cell number decreased in a time-dependent manner up to 240 h (Fig. 3A).

The cell cycle analysis shows that the number of HAK-1B cells at the S phase and G_2/M phase increased and decreased, respectively, with continuous contact of PEG-IFN-α2b, and this indicates the induction of S-phase arrest by PEG-IFN-α2b (Fig. 3B). In addition, the number of cells at the preG_1 phase increased with continuous contact of PEG-IFN-α2b, and this indicated the induction of apoptosis.

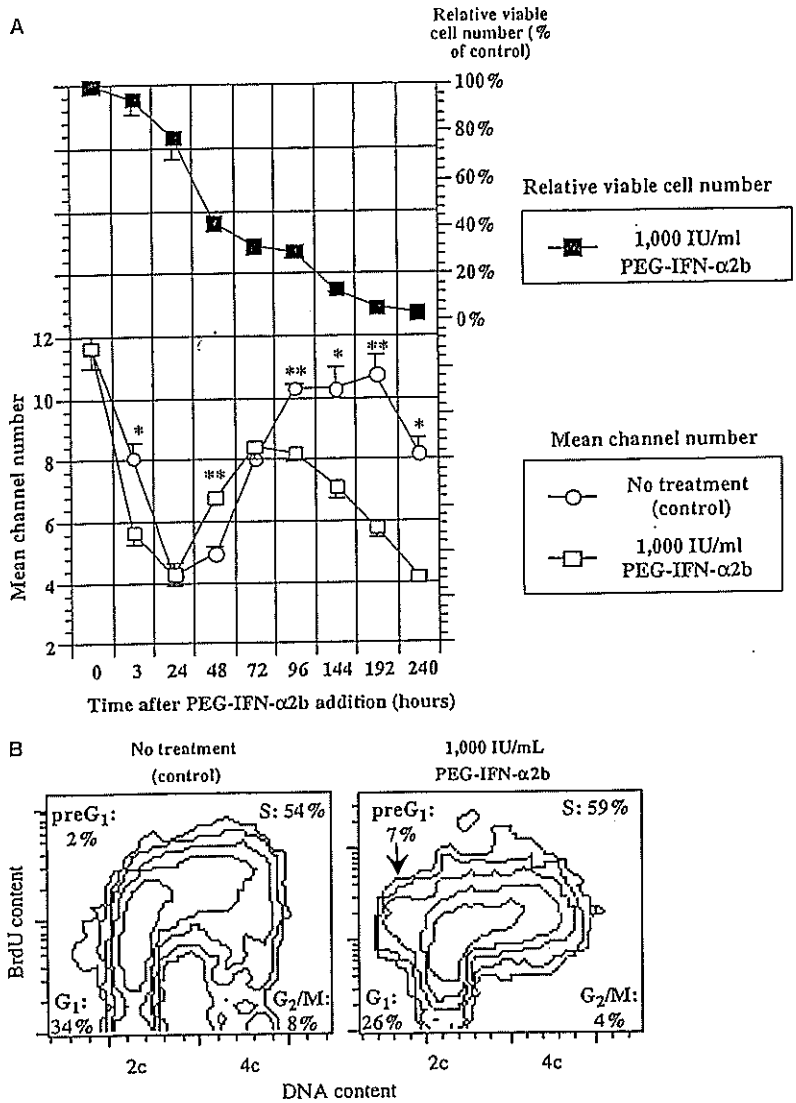

Fig. 3. Effects of 1000 IU/ml of pegylated IFN-α2b (PEG-IFN-α2b) on growth and IFN-α receptor-2 (IFNAR-2) expression in HAK-1B cells. (A) Time-course changes in relative viable cell number (% of Control) and IFNAR-2 expression before and after 1000 IU/ml of PEG-IFN-α2b addition. Cells reacted with anti-IFNAR-2 antibody or normal mouse IgG (control antibody) were stained with fluorescein isothiocyanate-conjugated goat anti-mouse immunoglobulin and analyzed using flow cytometry. The expression levels were compared according to the mean channel numbers that were calculated as the difference between the mean channel number in the cells stained with anti-IFNAR-2 antibody and that stained with normal mouse IgG (control antibody). The figures represent the average ± SE of at least two independent experiments, and each experiment used three to five samples for each measurement. $^{*}P<0.01$, vs continuous PEG-IFN-α2b contact. $^{**}P<0.001$, vs continuous PEG-IFN-α2b contact. (B) Cell cycle analysis. HAK-1B cells were cultured with 1000 IU/ml of PEG-IFN-α2b or medium alone (Control) for 72 h. The cells were labeled with 10 mM bromodeoxyuridine (BrdU) for 30 min, fixed, stained with anti-BrdU and propidium iodide, and analyzed using a FACScan. The contour plots are shown. The arrow shows the area of the $preG_1$ phase. The experiments were repeated twice, and almost identical results were obtained.

Effects of PEG-IFN-α2b on HCC cell proliferation in nude mice

Chronological changes in estimated tumor volume after subcutaneous injection of cultured HAK-1B cells to nude mice are summarized in Fig. 4. Dose-dependent suppression of tumor volume was observed in mice receiving PEG-IFN-α2b. In Experiment #1, a significant difference in the changes in tumor volume and tumor weight was observed between the Control mice and the mice that received 640, 6400, 64 000, or 640 000 IU of PEG-IFN-α2b or 6400 or 64 000 IU of IFN-α2b ($P<0.001$ by two-factor factorial ANOVA; and $P<0.05$–0.001 by the Mann–Whitney U-test) and between 64 000 IU of PEG- and non-PEG-IFN-α2b ($P<0.0001$ and $P<0.01$, Fig. 4 and Table 2). In Experiment #2, significant difference in tumor volume change was observed between the Control mice and the mice that received 640 or 6400 IU of PEG-IFN-α2b or 6400 IU of IFN-α2b and between 640 IU of

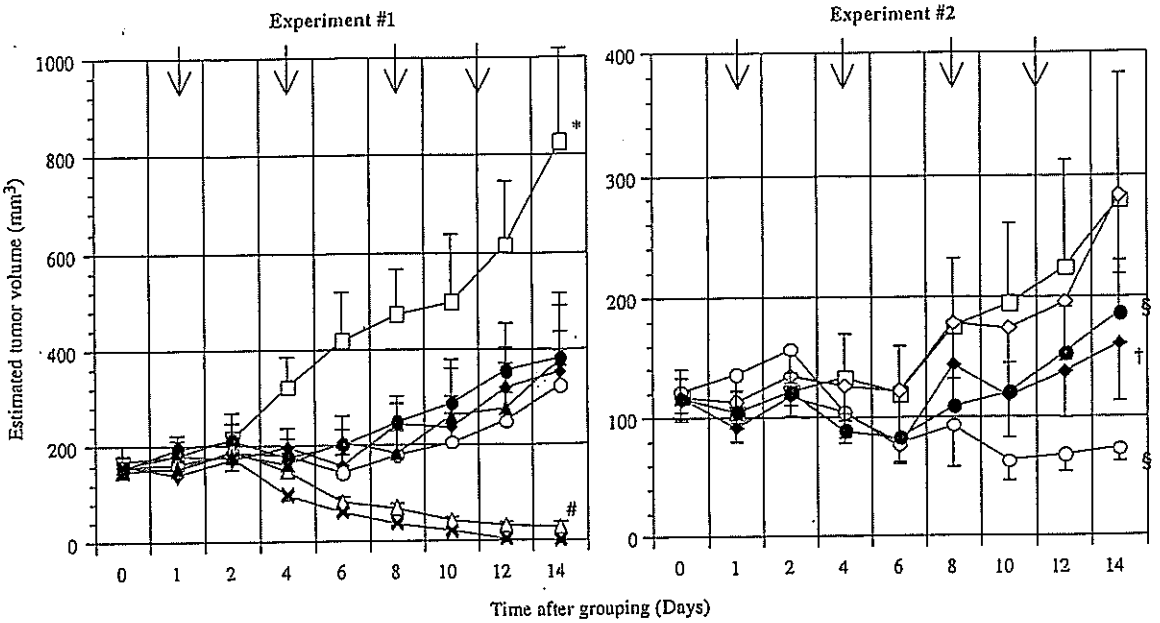

Fig. 4. Time-course change in estimated tumor volumes of subcutaneously transplanted human hepatocellular carcinoma tumors in nude mice. The mice received a subcutaneous injection of 640 (♦), 6400 (○), 64 000 (△), or 640 000 (✖) IU of pegylated IFN-α2b (PEG-IFN-α2b), or 6400 (●) or 64 000 (▲) IU of IFN-α2b, or medium alone (Control) (□) in Experiment #1, and of 640 (♦) or 6400 (○) IU of PEG-IFN-α2b, 640 (◇) or 6400 (●) IU of IFN-α2b, or medium alone (Control) (□) in Experiment #2, twice a week for two consecutive weeks. The arrows show the days of injection. *$P<0.001$, vs the other groups. #$P<0.0001$, vs IFN-α2b (64 000 IU). †$P<0.05$, vs control or IFN-α2b (640 IU). §$P<0.05$, vs Control. The experiments were repeated twice, and almost identical results were obtained. The figures represent average ± SE.

Table 2. Treatment of human HCC tumors subcutaneously transplanted in nude mice

Treatment group*	Number	Tumor weight (g)	Body weight (g)†
Experiment #1			
Control	8	0.436 ± 0.07‡	19.2 ± 0.6††
PEG-IFN-α2b (640 IU)	9	0.237 ± 0.05§	19.4 ± 0.4
PEG-IFN-α2b (6400 IU)	9	0.180 ± 0.03¶	19.9 ± 0.3
IFN-α2b (6400 IU)	6	0.259 ± 0.06§	19.4 ± 0.7
PEG-IFN-α2b (64 000 IU)	9	0.016 ± 0.01 ‖ ,#	19.0 ± 0.6
IFN-α2b (64 000 IU)	7	0.221 ± 0.06§	19.1 ± 0.5
PEG-IFN-α2b (640 000 IU)	9	0.0 ‖	19.6 ± 0.3
Experiment #2			
Control	8	0.160 ± 0.04	20.6 ± 0.5††
PEG-IFN-α2b (640 IU)	8	0.097 ± 0.02	20.1 ± 0.4
IFN-α2b (640 IU)	8	0.168 ± 0.03	20.7 ± 0.4
PEG-IFN-α2b (6400 IU)	7	0.050 ± 0.02¶	21.0 ± 0.3
IFN-α2b (6400 IU)	8	0.131 ± 0.03**	21.1 ± 0.3

*Cultured HAK-1B cells (1.0×10^7) were subcutaneously transplanted into nude mice. Five to seven days later when the largest diameter of the tumor reached approximately 5–10 mm, mice in each group were treated with twice per week sc injections of PEG-IFN-α2b, IFN-α2b, or culture medium. All mice were sacrificed on the 15th day. †Body weight on the 14th day. ‡Mean ± SE. §$P<0.05$ vs control. ¶$P<0.01$ vs control. ‖ $P<0.001$ vs control. #$P<0.01$ vs IFN-α2b (64 000 IU). **$P<0.03$ vs PEG-IFN-α2b (6400 IU). ††not significant vs the other groups. HCC, hepatocellular carcinoma; PEG-IFN-α2b, pegylated IFN-α2b.

PEG- and non-PEG-IFN-α2b ($P<0.05$, Fig 4). The tumors of the mice that received 6400 IU of PEG-IFN-α2b tended to be smaller in volume in both Experiments #1 and #2 ($P=0.068$ and 0.064, respectively), and the tumor was significantly lower in weight than that of IFN-α2b in Experiment #2 ($P<0.03$). At the end of the experiments, the estimated tumor volume in the mice that received 640 IU of PEG-IFN-α2b (3.2×10^4 IU/kg, about 1/3 of the clinical dose 9.6×10^4 IU/kg) in Experiments #1 and #2 became 42% and 58% of the Control, respectively. In the mice that received 640 000 IU of PEG-IFN-α2b, the tumors disappeared on the 14th day. PEG-IFN-α2b administration did not affect the body weight of the mice (Table 2).

Histological examination of the HAK-1B tumor specimens stained with HE revealed that the numbers of apoptotic cells in the mice treated with PEG-IFN-α2b (640–64 000 IU) or IFN-α2b (64 000 IU) were significantly higher than that of the Control, and the number increased dose dependently (Fig. 5A–C; Table 3). Immunostaining of vimentin fragment (V1) that is a marker for caspase-9 activation showed a positive reaction in the cytoplasm of the apoptotic cells (Fig. 5D).

No significant difference was observed in the number of blood vessels per unit area of the HAK-1B tumor between the Control and the PEG-IFN-α2b or IFN-α2b group (Table 3).

Immunohistochemical examination of BrdU uptake in HAK-1B tumors revealed that the BrdU labeling index was significantly higher in the Control than in the 6400 IU PEG-IFN-α2b or IFN-α2b groups (Fig. 5E, Table 3).

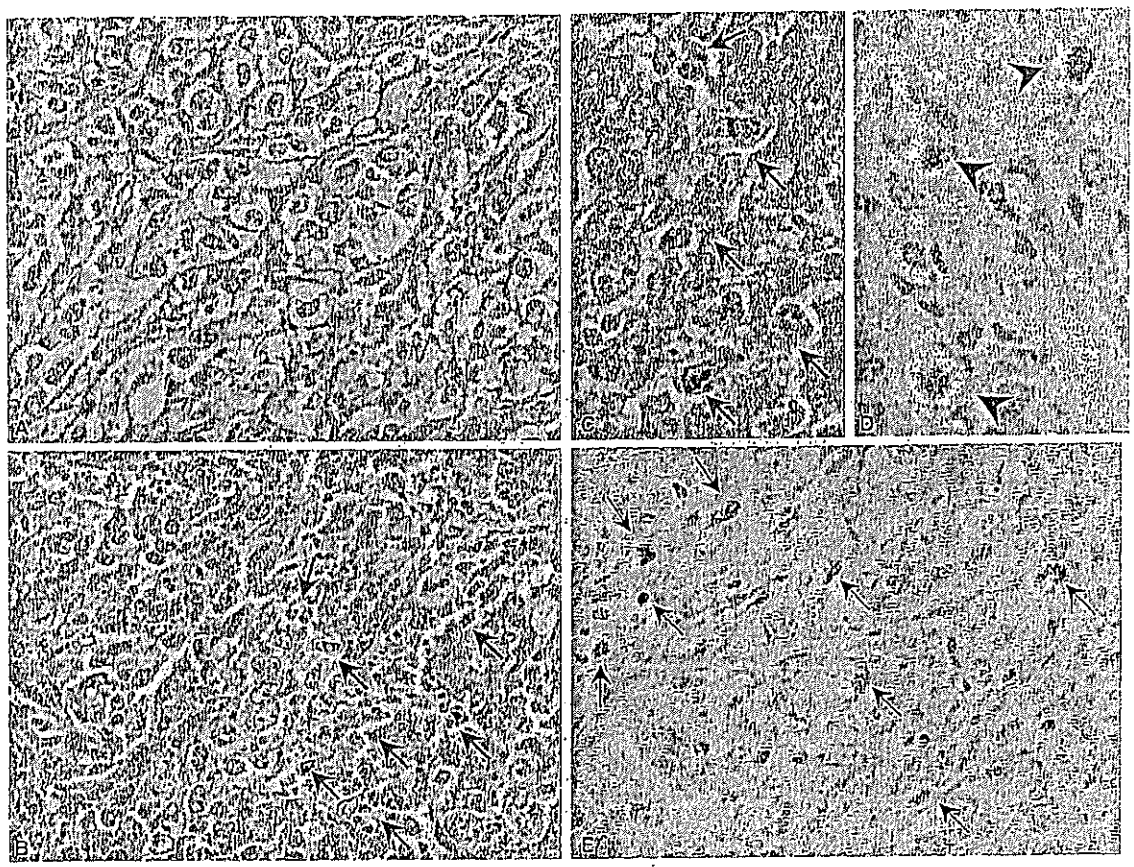

Fig. 5. Photomicrograph of subcutaneous human hepatocellular carcinoma tumor in nude mice that was developed after the injection of HAK-1B cells. (A) A control mouse that received culture medium alone. The tumor shows a thick trabecular arrangement of tumor cells and a sinusoid-like structure in the stroma. (B) A mouse that received a sc injection of 6400 IU pegylated IFN-α2b. There are many apoptotic tumor-cells (arrows, hematoxylin–eosin staining, × 200). (C) Higher magnification of B. It clearly shows apoptotic tumor cells characterized by shrinkage and eosinophilic change in the cytoplasm, chromatin condensation and/or fragmentation of nuclei (hematoxylin–eosin staining, × 400). (D) Immunostaining of vimentin fragment (V1). Positive reactions (red pigments) are shown in the shrunken cytoplasm of apoptotic cells as noted in C (counterstained with Mayer's hematoxylin, × 400). (E) Immunostaining of bromodeoxyuridine (BrdU). Many BrdU-positive cells (brown nuclear pigments) were found in a tumor of a control mouse (counterstained with Mayer's hematoxylin, × 200).

Table 3. Numbers of apoptotic cells, artery-like blood vessels, and BrdU-positive cells, and expression of IFNAR-2 subunit in human HCC tumors subcutaneously transplanted in nude mice

Treatment group*	Apoptosis†	Blood vessel‡	BrdU L.I.§	IFNAR-2¶
Experiment #1				
Control	21.3 ± 1.8 ‖	1.16 ± 0.20 ‖ ,**	15.5 ± 1.2 ‖	0.676 ± 0.10 ‖
PEG-IFN-α2b (640 IU)	28.4 ± 1.9#	1.04 ± 0.15	16.6 ± 3.1	0.410 ± 0.07#
PEG-IFN-α2b (6400 IU)	34.3 ± 5.0#	1.20 ± 0.19	10.2 ± 1.1#	0.451 ± 0.11
IFN-α2b (6400 IU)	24.0 ± 3.0	1.13 ± 0.16	9.4 ± 1.1#	0.656 ± 0.12
PEG-IFN-α2b (64 000 IU)	34.3 ± 5.3#	1.43 ± 0.39	ND	0.061 ± 0.06††
IFN-α2b (64 000 IU)	27.5 ± 2.5#	0.92 ± 0.20	10.6 ± 3.0	0.607 ± 0.11
PEG-IFN-α2b (640 000 IU)	ND	ND	ND	ND

*Cultured HAK-1B cells (1.0×10^7) were subcutaneously transplanted into nude mice. Five to seven days later when the largest diameter of the tumor reached approximately 5–10 mm, mice in each group were treated with twice per week sc injections of PEG-IFN-α2b, IFN-α2b, or culture medium. All mice were sacrificed on the 15th day. †The number of apoptotic cells was counted in ten 0.25 mm^2 areas in each section, and the average number per area in each group was obtained. ‡The number of the blood vessels in the tumor nodule was counted on each section, and the average number per area in each group was obtained. §The number of BrdU-positive cells was counted in ten 0.25 mm^2 areas in each section, and the average number per area in each group was obtained as the labeling index. ¶Values are expressed as pg/15 μg protein. ‖ Mean ± SE. #$P < 0.05$, vs control. **Not significant, vs the other groups. ††Not significant ($P = 0.068$) vs control. This is partly because only 2 samples were available for IFNAR-2 analysis in this group. BrdU, bromodeoxyuridine; IFNAR-2, IFN-α receptor-2; HCC, hepatocellular carcinoma; ND, not done; PEG-IFN-α2b, pegylated IFN-α2b.

The expression of the IFNAR-2 subunit tended to decrease in the PEG-IFN-α2b groups, and a significant difference was observed between the Control and the 640 IU PEG-IFN-α2b group ($P < 0.05$).

Discussion

PEG-IFN-α2b induced a time-dependent antiproliferative effect in 10 cell lines in contact with 4096 IU/ml of PEG-IFN-α2b for 24–96 h and a dose-dependent antiproliferative effect in nine cell lines *in vitro* in the range of 16 and 4096 IU/ml. On an antiviral unit basis, the antiproliferative activity of PEG-IFN-α2b was not significantly different from that of non-PEG-IFN-α2b *in vitro* based on IC50 values. Compared with BALL-1 IFN-α that consists of the α2 subtype (about 75%) and the α8 subtype (25%) or with IFN-αCon1, both PEG-IFN-α2b and IFN-α2b showed low antiproliferative activity in terms of relative viable cell number and IC50 (11, 12). This is consistent with our recent finding, i.e., that the antiproliferative activity of the IFN-α2 subtype *in vitro* is relatively weak compared with other IFN-α subtypes such as α5, α10 and α8 (32). As a mechanism of antiproliferation, apoptosis induction was observed in 9 cell lines that received 1000 IU/ml of PEG-IFN-α2b (morphological changes occurred in 10 cell lines with 4096 IU/ml). IFN-αCon1 that possesses the most potent antiproliferative effect among the three IFN-α preparations induced apoptosis in all 13 HCC cell lines at a similar concentration (12). The four cell lines (HAK-2, HAK-3, HAK-4, and KMCH-2) in which PEG-IFN-α2b did not induce a dose-dependent antiproliferative effect showed the highest IC50 values (> 100 000 IU/ml) to IFN-α2 subtype among the 13 cell lines (32) and showed resistance to PEG-IFN-α2b-mediated apoptosis (HAK-2, HAK-3, and KMCH-2) and/or low cell surface IFNAR-2 expression (HAK-3, HAK-4, and KMCH-2) (11).

When IFN-α binds to its receptors, the IFN-receptor-complexes are internalized and degradated intracellularly (33, 34). It was demonstrated that IFN-α down-regulates type I IFN receptors in peripheral blood mononuclear cells (PBMC, (35–37)). Nakajima et al. (36) reported that the number of IFN receptors on PBMC in patients with chronic hepatitis B decreased to about 50% of the baseline with a fivefold increase in 2′,5′-oligoadenylate synthetase activity when the patients were treated with IFN for 2 or 4 weeks. To date, however, there have been no studies on the down-regulation of IFN receptors and its relationship with the antiproliferative effects of IFN-α in liver cancer cells. Human type I IFN receptor consists of two subunits, IFNAR-1 and IFNAR-2. IFNAR-2 is the binding subunit and is more important than IFNAR-1 for the expression of IFN activity (3, 38, 39). Therefore, the current study chronologically examined the relationship between the antiproliferative effect and the expression of the IFNAR-2 subunit in HAK-1B cells up to 240 h after the addition of PEG-IFN-α2b. We chose HAK-1B for this study because this cell line expresses the highest IFNAR-2 subunit expression among the 13 liver cancer cell lines (11) and because this cell line was also selected for the *in vivo* experiment, allowing comparison of results in the *in vitro* setting with those *in vivo*. The expression of IFNAR-2 subunit was significantly down-regulated at 3 h compared with the Control and then significantly up-regulated at 48 h. Expression then decreased in a time-dependent manner after 72 h, and the viable cell number continuously decreased with time. The down-regulation of IFNAR-2 was the specific change because another cell surface protein, i.e., EGF receptor, was not down-regulated at 240 h compared with Control. Therefore, at least for the HCC cell line, HAK-1B, in an *in vitro* setting, the IFNAR-2 subunit is down-regulated but an efficient antiproliferative effect is induced with continuous contact with PEG-IFN-α2b. Lau et al. (35) studied the binding characteristics of IFN-α to PBMC in patients with chronic hepatitis B virus infection and reported a possible increase in binding affinity of the remaining receptors as a reason for the continuous effects of IFN-α in long-term IFN therapy that reduces the number of IFN-α receptors. On the other hand, Dooley et al. (40) reported a decrease in binding affinity. Therefore, this point also needs to be further studied on HAK-1B and other HCC cell lines.

We then examined the *in vivo* antitumor effects of PEG-IFN-α2b on mice. Twice-a-week administration of PEG-IFN-α2b dose-dependently suppressed the growth of sc transplanted human HCC. The growth was effectively suppressed even at 1/3 of the clinical dose in patients with chronic hepatitis C, and the tumor size was reduced to 42–58% of the Control. This antiproliferative effect was equivalent to the effect of a consecutive 14-day administration of an approximately 1.3 times larger clinical dose of IFN-αCon1 (12). The antiproliferative effect of PEG-IFN-α2b *in vitro* is lower than IFN-αCon1; therefore, our *in vivo* finding would be understood as the serum half-time of IFN-α2b becoming longer due to pegylation, then PEG-IFN-α2b at a high concentrations remaining in the serum for a long time to affect tumor cells, resulting in much stronger antitumor effects. This consideration is also supported by our results, i.e., PEG-IFN-α2b and IFN-α2b *in vitro* presented the same antiproliferative effects; however, *in vivo*, IFN-α2b presented significantly weaker antitumor